Ecological Modelling

Attributing hypoxia responses of early life Menidia menidia to energetic mechanisms with Dynamic Energy Budget theory
--Manuscript Draft--

Manuscript Number:	
Article Type:	VSI:DEB2023
Keywords:	Dynamic Energy Budget; DEBkiss; early life stages; Atlantic silverside; hypoxia; stressors
Corresponding Author:	Teresa Grace Schwemmer, Ph.D. Stony Brook University School of Marine and Atmospheric Sciences South Kingstown, RI UNITED STATES
First Author:	Teresa G. Schwemmer, Ph.D.
Order of Authors:	Teresa G. Schwemmer, Ph.D.
	Roger M. Nisbet, Ph.D.
	Janet A. Nye, Ph.D.
Abstract:	Highlights • Bioenergetic mechanisms of Atlantic silverside hypoxia responses were investigated. • Hypoxia effects were modeled with a simplified Dynamic Energy Budget model. • We connected physiology with energetic processes to identify potential mechanisms. • Conversion efficiency and mortality parameters best explained hypoxia effects. • This mechanism could impact energy flow across generations and trophic levels.
Suggested Reviewers:	Benjamin Martin University of Amsterdam Department of Theoretical and Computation Ecology b.t.martin@uva.nl Expertise in DEB models of fish, hypoxia and metabolism research, has used a DEBkiss model.
	Tjalling Jager DEBtox Research tjalling@debtox.nl Extensive expertise and experience with DEB modeling, developed the DEBkiss model, and has used it to model environmental stressor effects.
	Laure Pecquerie Université de Brest laure.pecquerie@ird.fr Expertise in DEB models of fish, fish metabolism and growth.
	Nina Marn Ruđer Bošković Institute nina.marn@irb.hr Expertise in DEB theory, physiology and energetics.
Opposed Reviewers:	

Dr. Teresa G. Schwemmer, Ph.D.
Stony Brook University
Stony Brook, NY 11794-5000
teresa.schwemmer@gmail.com

March 29, 2024

Dr. Hsiao-Hsuan Wang, Ph.D.
Editor-in-Chief
Ecological Modelling

Dear Dr. Wang:

I am writing to submit our manuscript entitled "Attributing hypoxia responses of early life *Menidia menidia* to energetic mechanisms with Dynamic Energy Budget theory" for your consideration as a Research Article in *Ecological Modelling*, in the special issue "Metabolic organization across scales of space and time".

We used a simplified Dynamic Energy Budget model (DEBkiss) to understand the mechanisms responsible for responses of Atlantic silverside (*Menidia menidia*) to hypoxia, an ecological stressor that is intensifying globally. This study expands on previous experimental work on Atlantic silversides that documented reduced early life growth, hatching success, and survival when reared under environmentally relevant levels of hypoxia. To connect these whole-organism responses to the energy budget, we employed the concept of synthesizing units (SU) to derive an oxygen-dependent correction factor that treats hypoxia as an inhibiting or damaging agent – a novel application of the SU concept. We identified conversion efficiency for growth and stage-specific mortality rates as the most likely DEB processes responsible for the experimentally observed responses to hypoxia.

This work will be of great interest to the readers of *Ecological Modelling* and this special issue because it takes a novel approach to modeling impacts of the real-world problem of intensifying hypoxia with a widely applicable DEB model. This model is a valuable tool to supplement ecological stressor experiments, particularly in early life stages when laboratory procedures are logistically constrained. Our results suggest that damage to the SUs, likely by anaerobic byproducts such as lactate, reduced the efficiency of growth and development, which could lead to lower recruitment and fecundity in realistic hypoxia scenarios. Readers will be interested in the implications of our findings using a model at the organismal scale of organization for population and ecosystem dynamics, as well as our suggestions for future work to refine the model using suborganismal data linked to physiological modes of action.

All authors have seen and approved the manuscript for submission to *Ecological Modelling* and have agreed to abide by the Editorial Policy. The authors confirm that this manuscript is original research that has not been previously published and is not under consideration for publication elsewhere. A previous version of this work is published only in my Ph.D. thesis and subsets of

our findings have been presented at the following conferences: the 2023 Dynamic Energy Budget Symposium in Baton Rouge, LA; the 2022 Larval Fish Conference in San Diego, CA; the 2021 Dynamic Energy Budget Symposium (virtual); and the 2021 American Fisheries Society meeting in Baltimore, MD.

Thank you for your time and consideration. I look forward to your response.

Sincerely,

Teresa G. Schwemmer, Ph.D.
Corresponding Author

Highlights for Schwemmer et al.

"Attributing hypoxia responses of early life *Menidia menidia* to energetic mechanisms with Dynamic Energy Budget theory"

Highlights

- Bioenergetic mechanisms of Atlantic silverside hypoxia responses were investigated.
- Hypoxia effects were modeled with a simplified Dynamic Energy Budget model.
- We connected physiology with energetic processes to identify potential mechanisms.
- Conversion efficiency and mortality parameters best explained hypoxia effects.
- This mechanism could impact energy flow across generations and trophic levels.

Attributing hypoxia responses of early life *Menidia menidia* to energetic mechanisms with Dynamic Energy Budget theory

Teresa G. Schwemmer[a,1], Roger M. Nisbet[b], and Janet A. Nye[c]

[a]School of Marine and Atmospheric Sciences, Stony Brook University, Stony Brook, NY 11794, U.S.A., teresa.schwemmer@gmail.com
[b]Department of Ecology, Evolution and Marine Biology, University of California Santa Barbara, Santa Barbara, CA 93106, U.S.A., rogernisbet@ucsb.edu
[c]Institute of Marine Sciences, University of North Carolina at Chapel Hill, Morehead City, NC 28557, U.S.A., jnye@nyelab.org

[1]Corresponding author, present affiliation: Teresa G. Schwemmer, Mid-Atlantic Coastal Acidification Network, Newark, DE 19716, U.S.A., teresa.schwemmer@gmail.com

Highlights

- Bioenergetic mechanisms of Atlantic silverside hypoxia responses were investigated.
- Hypoxia effects were modeled with a simplified Dynamic Energy Budget model.
- We connected physiology with energetic processes to identify potential mechanisms.
- Conversion efficiency and mortality parameters best explained hypoxia effects.
- This mechanism could impact energy flow across generations and trophic levels.

Abstract

Ocean deoxygenation is intensifying worldwide due to warming and eutrophication, particularly in estuaries and coastal waters. Although the Atlantic silverside (*Menidia menidia*) is tolerant of the fluctuating environmental conditions in its estuarine habitat, chronic hypoxia impairs hatching, growth, and survival in the early life stages. We used a simplified version of a Dynamic Energy Budget model (DEBkiss) to test the hypothesis that experimentally observed changes in animal performance can be explained by one or more of the rate processes in the model. We sought to identify the DEBkiss parameters that, when adjusted with a correction factor based on inhibition of Synthesizing Units, provided the best fit to hypoxia effects in the three state variables of total length, egg buffer mass, and survival over time. Because hypoxia reduces survival in embryos and newly hatched larvae, we added a survival state variable controlled by pre- and post-hatching mortality parameters. Applying the hypoxia effects to reduce the conversion efficiency of assimilates to structure accounted for some of the hypoxia-related changes in all three state variables. However, the best fit was achieved by simultaneously reducing the conversion efficiency and increasing both mortality parameters. In contrast, changing the parameter for maintenance rate with hypoxia provided little to no improvement of fit to the data. Reduced conversion efficiency under hypoxia would suggest that less of the energy invested by parents and consumed through predation is converted into biomass in *M. menidia* offspring, with implications for size at age that could threaten recruitment and alter the flow of energy through the food web.

2

71

1. Introduction

Hypoxia is common in coastal and estuarine waters and is expected to intensify with global warming (Diaz and Rosenberg, 2008; Breitburg et al., 2018). Between anthropogenic influence on nearshore waters and the natural dynamics of shallow, partially enclosed water bodies, hypoxia often co-occurs with other stressors such as high temperature, ocean acidification, and pollutants (Gruber, 2011). In temperate estuaries, stratification and productivity associated with high temperatures in spring and summer cause hypoxic and eutrophic zones to form and great fluctuations in dissolved oxygen (DO) on diel to monthly time scales (O'Donnell et al., 2004; Baumann and Smith, 2018; Testa et al., 2018). While fish species that currently live in such areas tend to have mechanisms to cope with episodic hypoxia (Farrell and Brauner, 2009; Zhu et al., 2013; Baumann, 2019), these are not necessarily adequate for tolerance of longer duration events. Fishes that spawn in the spring and summer may be particularly vulnerable because they are exposed to hypoxia during the sensitive early life stages. Embryos and young larvae rely largely on diffusion for oxygen uptake and lack well-developed mechanisms, such as high surface area gills, to meet oxygen demands in low DO water (Rombough, 1988). While later stage fishes and even some early larvae can swim to avoid hypoxic habitats (Niklitschek and Secor, 2005; Chapman and McKenzie, 2009), embryos cannot utilize this response. Mortality can result directly from severe hypoxia or indirectly from reduced growth increasing susceptibility to predation. Even fish that survive may incur sublethal effects with lasting, lifelong consequences for growth, development, and reproduction (Stierhoff et al., 2006; Vanderplancke et al., 2015; Zambonino-Infante et al., 2017). Modeling the energetic mechanisms of responses to hypoxia using unified principles on model species can help connect physiology and life history to population-level changes and serve as a valuable alternative and/or supplement to time- and labor-intensive laboratory experiments on other species, particularly with very small embryos and larvae.

Hypoxia is known to inhibit growth and survival in early life fishes (Rombough, 1988; Cross et al., 2019; Del Rio et al., 2019), as oxygen is required for the processes that maintain homeostasis and convert food for growth and activity. Anaerobic energy production fuels these processes with about $1/15^{th}$ the ATP yield of aerobic respiration. Hypoxic exposure may lead to physiological responses such as depressed metabolism (Richards, 2009; Schwemmer, 2023),

102 limited growth, increased ventilation, and changes to hematocrit, hemoglobin, and erythrocyte

103 quantities and characteristics (Taylor and Miller, 2001; Stierhoff et al., 2009; Bianchini and

104 Wright, 2013). Metabolism has also been shown to increase after temporary hypoxia as fish

105 remove lactate accumulated from anaerobic respiration (Heath and Pritchard, 1965).

106 　　　　Hypoxia often has interactive effects with other stressors such as temperature (Brandt et

107 al., 2009; McBryan et al., 2013; Earhart et al., 2022) and high carbon dioxide (CO_2; Hancock and

108 Place, 2016; Miller et al., 2016; Morrell and Gobler, 2020). The Atlantic silverside (*Menidia*

109 *menidia*) is an estuarine forage fish that has frequently been used as a model species to

110 understand interactive effects of high CO_2 and hypoxia (DePasquale et al., 2015; Miller et al.,

111 2016; Murray and Baumann, 2018; Schwemmer et al., 2020). Rearing *M. menidia* offspring in

112 static low DO significantly delayed hatching, reduced survival to hatching and larval survival,

113 and reduced embryo and larval growth (Cross et al., 2019). However, the negative effects of both

114 hypoxia and high CO_2 were mitigated when offspring were exposed to diel-fluctuating

115 treatments rather than static (Cross et al., 2019). While diel fluctuations are a realistic

116 representation of current changes in community photosynthesis and respiration between day and

117 night, environmental change in coming years could extend hypoxic duration to reduce periods of

118 relief. Warming reduces oxygen solubility while increasing metabolic rates of organisms that

119 draw down oxygen when densely aggregated. At the same time, higher summer temperatures and

120 freshwater input in some regions will intensify stratification that separates low-oxygen water

121 from surface oxygen diffusion (Rabalais et al., 2009; Howarth et al., 2011). Currently *M.*

122 *menidia* is tolerant enough that population declines are not a concern, but without knowledge of

123 the mechanisms of early life impacts it is hard to anticipate whether this will change under

124 intensifying deoxygenation or with additional stressors (Baumann, 2019).

125 　　　　Dynamic Energy Budget (DEB) theory is a bioenergetic framework designed to bridge

126 multiple levels of biological organization in assessing stressor effects and their mechanisms in a

127 vast variety of species (Kooijman, 2010a; AmP, 2023). This approach follows energy allocation,

128 represented in suborganismal metabolic fluxes, and how it leads to life history outcomes such as

129 growth rate, reproductive output, and survival, using physical and biological concepts that are

130 generalizable to most species (Jusup et al., 2017). It accounts for differences in the energy budget

131 at each stage to allow modeling of life stage transition timing and stage-specific responses to

132 stressors (Kooijman, 2010a). DEB theory is often used to connect experimental observations of

4

multiple stressor effects to both the underlying energetic mechanisms (Kooijman, 2018) and life history outcomes that feed into population dynamics (Nisbet et al., 2000; Martin et al., 2013; Smallegange et al., 2017). It is important to connect suborganismal and organismal responses to population implications because targeted conservation actions typically operate at this level, but this scaling requires additional steps and remains a challenge (but see Nisbet et al., 1989; Martin et al., 2013; Grear et al., 2020; Tai et al., 2021). The ability to bridge levels of biological organization from the molecular to population level makes DEB theory an excellent tool for enhancing the utility of experimental hypoxia data for conservation and management (Lavaud et al., 2021).

Depending on the application and types of data available, simplified versions of the standard DEB model can be used (e.g. Kooijman and Metz, 1984; Jager, 2018; Martin et al., 2017). Although complexity can sometimes be beneficial (Evans et al., 2013), simple parameter-sparse models are often preferable for their predictive power and ability to be applied, tested, and interpreted widely (Holling, 1966; May, 2001; Jusup et al., 2017). The DEBkiss framework (Figure 1) is a moderately simplified variation on the standard DEB model for animals that eliminates explicit representation of reserve and assumes that assimilates are immediately allocated to structure, maintenance, and reproduction (Jager et al., 2013). This reduces the data requirements, the role of compound parameters, and, depending on the data, the total number of parameters to be estimated (Jager et al., 2013). The simplicity of DEBkiss makes it ideal for adaptation to many species of ecological or commercial value, even when the existing studies were not originally intended for this use.

156
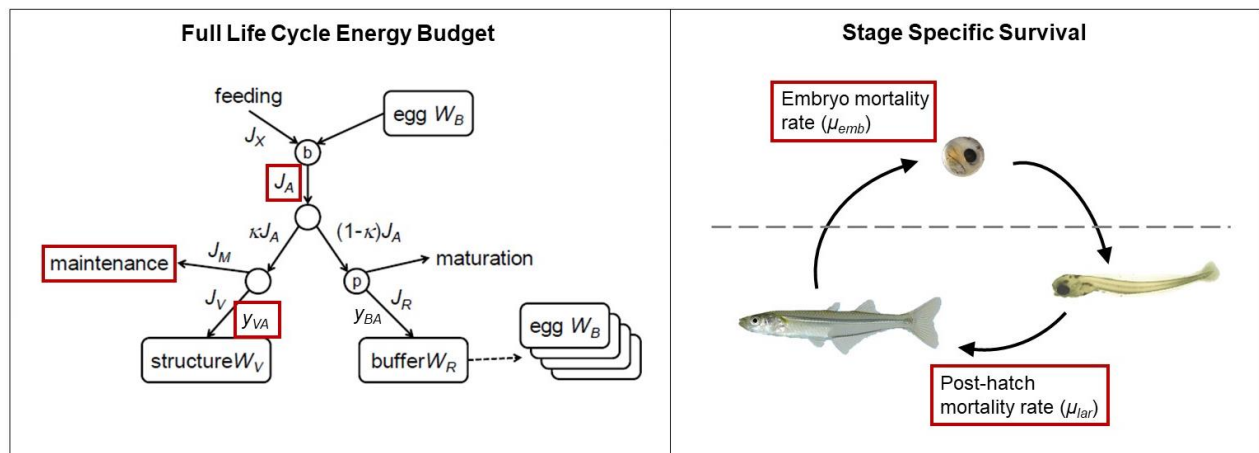
Figure 1. Conceptual diagram of the DEBkiss model highlighting parameters of interest for hypoxia effects. The DEBkiss model (diagram adapted from Jager et al., 2013) used in this study includes stage-specific survival parameters. The hypothesized parameters for hypoxia stress mechanisms are highlighted in red boxes. The left panel shows the energy budget for the full life cycle and the right panel shows how the stage-specific survival modification is applied to embryos, larvae, and adults of *M. menidia*.

Romoli et al. (2024) present a detailed comparison of the advantages and limitations for ecological risk assessment of a model based on DEBkiss versus a model based on Kooijman's "standard" DEB model. The comparison focuses on application in ecotoxicology but the reasoning carries over to other forms of environmental stress, including this study on hypoxia. They highlight several "modeling choices" that should influence the choice of approach, including: (i) insufficient information in data sets; (ii) capturing differences between data sets for the same species; and (iii) auxiliary hypotheses. Consideration of each of these led us to choose DEBkiss for our work after much unsuccessful effort attempting to interpret parameter estimates with the standard model (using the Add-my-Pet software; AmPtool, 2022; Marques et al., 2018).

We used DEBkiss to test the hypothesis that changes in animal performance under hypoxia can be explained by changes in one or more of the rate processes in the model, and to identify the bioenergetic mechanisms underlying experimental hatching, growth, and survival effects of hypoxia in early life stages of *M. menidia* observed in Cross et al. (2019). First, we fit the DEBkiss model to full-life data on total length, reproductive output, hatch timing, and survival and estimated or calculated parameters under fully oxygenated conditions. Second, we used the concept of Synthesizing Units (SU) that are inhibited or damaged by hypoxia to directly or indirectly change key parameters in the DEBkiss model (Muller et al 2019). SUs are generalized enzymes that produce products such as body structure or support maintenance requirements from incoming fluxes of substrate, i.e. food or egg buffer (Kooijman, 1998; Kooijman, 2010a). With single substrates for each life stage the SU formalism is equivalent to standard Michaelis-Menten kinetics, but the SU interpretation allowed us to exploit the subtleties in describing inhibition set out by Muller et al. (2019). We used a correction factor based on

187 inhibition or damage to the SU to fit the model to early-life data for four DO treatments. We

188 evaluated which parameter or combination of parameters, when adjusted with the correction

189 factor, was able to best account for the full set of hypoxia responses observed in experiments and

190 thus allow inference of mechanism.

191

2. Methods

2.1. DEBkiss Model Description

194   The material flows are shown in Fig. 1. The yolk in an egg is treated as a buffer of "food"

195 for the developing embryo that initially has an infinitesimally small structural biomass. There is

196 no reserve compartment between food assimilation and its utilization. Hatching occurs when the

197 egg buffer is fully depleted. After hatching, juveniles feed and assimilated food is allocated to

198 growth and maintenance versus maturity or reproduction in accordance with the κ-rule.

199   The DEBkiss assumptions and equations are from Jager (2018). The parameters are

200 defined in Table 1 and the variables, differential equations, and conversions are defined in Table

201 2. The flux of food or, for embryos, from the egg buffer (W_B) is immediately converted to

202 assimilates which are allocated to a somatic fraction (κ) and a reproductive fraction ($1-\kappa$; Figure

203 1). The assimilation flux (J_A) is the product of the scaled measure of resource availability (f), the

204 volumetric surface area (L^2), and the parameter maximum area-specific assimilation rate (J^a_{Am})

205 where $f = 1$ for embryos and for post-hatching fish fed *ad libitum*. Within the somatic branch, a

206 flux to maintenance (J_M) is prioritized while the remainder goes to structural mass (J_V) with a

207 conversion efficiency y_{VA}. The maintenance flux is proportional to structure.

208

Parameter	Symbol	Fixed or estimated	Value
Max. area-specific assimilation rate	J^a_{Am}	Estimated	0.333 mg mm^{-2} d^{-1}
Max. volume-specific maintenance rate	J^v_M	Fixed	0.0214 mg mm^{-3} d^{-1}
Initial egg buffer mass	W_{B0}	Fixed	0.15 mg
Total length at puberty	L_{Vp}	Fixed	102 mm
Yield of assimilates on volume	y_{AV}	Fixed	0.8
Yield of egg buffer on assimilates	y_{BA}	Fixed	0.95
Yield of structure on assimilates	y_{VA}	Estimated	0.365
Fraction of assimilates allocated to soma	κ	Fixed	0.8
Scaled food level	f	Fixed	1
Scaled food level for embryo	f_B	Fixed	1
Mortality rate for embryos	μ_{emb}	Estimated	0.0639

7

Mortality rate for larvae	μ_{lar}	Estimated	0.0294

209 **Table 1. DEBkiss parameters, their abbreviations, and their fixed or estimated values from**

210 **fitting to full life data.** Units are given with the value unless the parameter is a unitless ratio.

211

212

Flux	Symbol	Equation	Units
Assimilation flux	J_A	$J_A = f\, J_{Am}^a\, L^2$	mg day^{-1}
Maintenance flux	J_M	$J_M = J_M^v\, L^3$	mg day^{-1}
Flux to structural growth	J_V	$J_V = y_{VA}\,(\kappa\, J_A - J_M)$	mg day^{-1}
Flux to reproduction buffer	J_R	$J_R = (1-\kappa)\,J_A - J_J$ when $W_V \geq W_{Vp}$ $J_R = 0$ when $W_V < W_{Vp}$	mg day^{-1}
Flux to maturity	J_J	$J_J = J_J^v L^3$ when $W_V < W_{Vp}$ $J_J = J_J^v L_{Vp}^3$ when $W_V \geq W_{Vp}$	mg day^{-1}
State Variable	**Symbol**	**Equation**	**Units**
Structural dry mass over time	W_V	$\dfrac{dW_V}{dt} = J_V$	mg day^{-1}
Continuous reproduction rate	R	$\dfrac{dR}{dt} = \dfrac{y_{BA}\, J_R}{W_{B0}}$	eggs day^{-1}
Egg buffer (yolk) mass	W_B	$\dfrac{dW_B}{dt} = -J_A$	mg day^{-1}
Survival	S	$\dfrac{dS}{dt} = -\mu_{emb}\, S$ when $W_B > 0$ $\dfrac{dS}{dt} = -\mu_{lar}\, S$ when $W_B = 0$	unitless (range 0-1)
Other variables and conversions	**Symbol**	**Equation**	**Units**
Total physical length	L^M	$L^M = \dfrac{L}{\delta_M}$	mm
Volumetric length	L	$L = \sqrt[3]{L^3}$	mm
Shape coefficient	δ_M	$\delta_M = \dfrac{L}{L^M}$	unitless
Dry weight density of structure	d_V	$d_V = \dfrac{W_V}{L^3}$	mg mm^{-3}
Dry mass at puberty	W_{Vp}	$W_{Vp} = d_V * (L_{Vp} * \delta_M)^3$	mg
Volume-specific maturity maintenance costs	J^v_J	-	mg mm^{-3} day^{-1}
Structural volume at puberty	L_{Vp}^3	-	mm^{-3}

8

| Scaled measure of resource availability | f | - | unitless (range 0-1) |

213 **Table 2. Model definition.** Fluxes, state variables, and differential equations in the DEBkiss

214 model.

215

216   For juveniles, the non-somatic fraction of assimilates is spent on maturation, or

217 increasing complexity. While the standard DEB formulation uses a state variable for maturity

218 that triggers changes between life stages, DEBkiss instead uses a constant size at puberty to

219 specify when reproduction is initiated (Kooijman, 2010b; Jager et al., 2013), so the maturity

220 variable plays no role in the current work. Once the mass at puberty is reached (W_{Vp}),

221 reproductive flux (J_R) toward egg production begins in adults with a conversion efficiency y_{BA}.

222 Although *M. menidia* have a distinct larval and juvenile stage, we treated both as the juvenile

223 stage because the relevant aspects of their energy budget for DEBkiss are assumed to be

224 identical.

225   Because our growth data are in total length, we used a shape correction coefficient (δ_M)

226 and dry weight density (d_V) to connect length with the model state variables (Table 2). We

227 calculated these constants using data on *M. menidia* length and egg volume (Klahre, 1997) and a

228 total length (L^M) to dry weight (W_V) conversion (H. Baumann, personal communication):

$$W_V = e^{(2.997*\ln(L^M)-6.7)} \tag{1}$$

230 After calculating W_V from $L^M = 5.3$ mm at hatching (Cross et al., 2019), we obtained a dry

231 weight at hatching of 0.18 mg. Assuming there is negligible change in weight or volume during

232 hatching, we used the volume of an egg immediately before hatching, $L^3 = 0.45$ mm^3, to

233 calculate d_V using:

$$d_V = \frac{W_V}{L^3} \tag{2}$$

235 This gave us $d_V = 0.4$ mg mm^{-3}. We similarly used the egg volume to calculate volumetric length

236 of an embryo as $L = 0.77$ mm, which gives us a δ_M of 0.145 using the following equation:

$$\delta_M = \frac{L}{L^M} \tag{3}$$

238 However, this value led the model to underestimate total length later in the life span, suggesting

239 the δ_M value was too high for this long and slender fish. We manually adjusted δ_M to a final value

240 of 0.107 which provided a reasonable fit to length data and a better starting point for parameter

241 estimation.

242   We added a survival state variable (S) which, in addition to allowing an alternative

243 outcome to hatching, enabled us to model survival as a consequence of hypoxia effects on the

244 energy budget. We fit mortality parameters for embryos and post-hatch fish (μ_{emb} and μ_{lar}) to data

245 for survival to hatching and larval/juvenile survival (Figure 1; Table 2). In our implementation of

246 survival, the only DEB process influencing survival is egg buffer depletion, which determines

247 the time to hatch and thus when the embryo mortality rate switches to the post-hatch mortality

248 rate. This means survival is indirectly affected by the assimilation rate and conversion efficiency

249 of assimilates into structure.

250

251   *2.2. Data*

252   We calculated and estimated DEBkiss parameters in normoxic conditions (Section 2.3)

253 and modeled hypoxia effects (Section 2.5) based on four types of data: total length over time,

254 egg buffer mass over time (extrapolated from knowledge of egg mass and age at hatching),

255 cumulative egg production over time, and proportion surviving since fertilization over time. As

256 described in the introduction, the data available for this model led us to use DEBkiss over the

257 "standard" DEB model based on the factors highlighted by Romoli et al. (2024). We had

258 insufficient data, had to integrate information from multiple studies of the same (and similar)

259 species, and had to hypothesize plausible values for a few parameters.

260   Data for total length were sourced from four studies. Length at hatching and 15 days

261 post-hatching (dph) came from a study that reared *M. menidia* offspring in different static

262 oxygen levels across two experiments (Cross et al., 2019). This provided data for parameter

263 estimation at control oxygen levels described in Section 2.3 and modeling three reduced oxygen

264 treatments (Section 2.5 and Table 2). We sourced additional length data for the full life span

265 from control levels of experiments that exposed *M. menidia* offspring to ambient and elevated

266 CO_2 levels (Murray and Baumann, 2018; Murray and Baumann, 2020; Concannon et al., 2021).

267 All total length data were obtained from fish maintained in static laboratory conditions at 24°C.

268   Data for the state variables of egg buffer mass (via time to hatching, when egg buffer

269 mass is zero), as well as survival at hatching and at 15 dph, were obtained from Cross et al.

270 (2019). The control data from these experiments were used to estimate parameters under

271 normoxia (Section 2.3). We also obtained normoxic survival data from a study on the effects of

272 temperature and CO_2 on *M. menidia* early life survival, using only the 24°C and control CO_2 data

273 (Murray and Baumann, 2018). Four additional data points for long-term survival in laboratory

274 conditions at 17°C were obtained from a study that exposed *M. menidia* offspring until 122 dph

275 to two CO_2 levels, of which we only used data from the control level (Murray et al., 2017).

276 Lastly, the data for cumulative egg production over time, used to estimate parameters under

277 normoxia (Section 2.3), were also obtained from control groups in Concannon et al. (2021), a

278 study in which wild-caught juveniles were held in the laboratory at 20°C in different CO_2

279 treatments and strip-spawned once they reached reproductive maturity.

280

281 *2.3. Parameter estimation under normoxia*

282 We estimated four parameters by fitting them to full-lifespan data listed in Section 2.2

283 (J^a_{Am}, y_{VA}, μ_{emb}, and μ_{lar}), calculated four parameters from data (J^v_M, W_{B0}, L_{Vp}, and f), and fixed at

284 suggested values parameters for which we had insufficient data to calculate or estimate (y_{AV}, y_{BA},

285 κ, and f_B; Jager, 2018). The primary parameters and their calculated or estimated values are

286 found in Table 1. Fitting was done in Matlab with the platform BYOM v.6.4 and the package

287 DEBkiss v.2.3a (https://www.debtox.info/byom.html). BYOM uses a Nelder-Mead simplex

288 search to optimize the parameters for a set of ordinary differential equations by minimizing

289 negative log-likelihood (NLL). The DEBkiss package works under BYOM to estimate model

290 parameters based on their effect on the DEBkiss equations and the auxiliary equations. The

291 differential equations predict length, egg production, egg buffer mass, and survival over time

292 with the differences from observations used to calculate NLL.

293 Before estimating any parameters with the optimization described above, we ran

294 simulations with fitting turned off using a set of recommended parameters (Jager, 2018) and

295 parameters we calculated from data on *M. menidia*, as described below. We visually assessed fit

296 and noted the NLL calculated from each simulation as we adjusted parameters to obtain a

297 reasonable set of initial parameters before estimating any. Testing a range of parameters and

298 obtaining realistic initial parameters helps avoid detecting local minima with the optimization.

299 This also helped us reduce the number of parameters being estimated to avoid overfitting and so

300 that there were not multiple correlated parameters free at once. Furthermore, we were able to

301 obtain a reasonable fit using suggested values for y_{AV}, y_{BA}, and κ for unstressed fish that are

302 thought to be widely applicable across species (Lika et al., 2011; Jager, 2018). The suggested

303 value for y_{VA} of 0.8 from the literature (Lika et al., 2011; Jager, 2018) did not allow a realistic fit

304 to the length data, but the length, reproduction, and egg buffer depletion data allowed it to be re-

305 estimated with the BYOM optimization. Ultimate length was used to fit J^a_{Am} to a reasonable

306 value while fixing all other parameters before estimating y_{VA}, because both parameters affect

307 growth and egg buffer depletion in the model and therefore cannot be estimated simultaneously.

308 Finally, we used the BYOM optimization to estimate μ_{emb} and μ_{lar}.

309 The length and reproductive data allowed us to calculate "length at puberty" (L_{Vp}),

310 defined as the length at which egg production begins. We obtained W_{B0} from *M. menidia* egg dry

311 weight data (Klahre, 1997) and calculated δ_M and d_V from total length, egg diameter, and egg

312 mass data (Cross et al., 2019; Klahre, 1997; Concannon et al., 2021). To calculate volume-

313 specific maintenance costs (J^v_M), we used data on the rate of decrease in larval dry weight over a

314 period of starvation in the congeneric species *M. beryllina* (Letcher and Bengtson, 1993).

315 Borrowing from closely related species is a common practice in bioenergetic modeling when the

316 species has similar habitat, life history, and physiology (Sibly et al., 2013). *M. menidia* and *M.*

317 *beryllina* have overlapping habitats and similar life history, egg sizes, and body sizes, although

318 *M. beryllina* reaches a smaller ultimate length (Middaugh, 1981; Bengtson, 1984; Middaugh and

319 Hemmer, 1992). All *M. menidia* experiments used in this study fed fish *ad libitum* in all

320 treatment levels, so *f* was set to 1. For studies that exposed fish to different CO_2 levels, we only

321 used data from control groups to avoid potential CO_2 effects in the data.

322

323 *2.4. Relating DEB processes to physiology*

324 We aimed to identify the DEBkiss parameters responsible for observed whole-organism

325 effects of rearing *M. menidia* in hypoxia by applying a correction factor to modify one or more

326 parameters with decreasing oxygen based on inhibition of or damage to a SU. Although oxygen

327 can be a limiting substrate in SUs, previous work suggests that *M. menidia* embryos only become

328 metabolically oxygen-limited below a critical level of 2.04 mg L^{-1} (Schwemmer, 2023), while it

329 remains oxygen-independent at the treatments for which we have data (2.7, 3.1, 4.2, and 7.7 mg

330 L^{-1}; Schwemmer et al., 2020). We therefore considered a single-substrate growth SU in which

331 food or egg buffer was the substrate. The mathematical characterization of inhibition and damage

332 is in Section 2.5.

333 Inhibiting agents reversibly bind to SUs, preventing them from accepting substrates to

334 proceed with their reaction. Damage, in contrast, induces dysfunction that is irreversible upon

12

335 removal of the damaging agent; however, damaged SUs can be repaired or replaced (Muller et

336 al., 2019). The idea is that hypoxia induces the production of compounds that in turn bind to

337 SUs. We used existing information on the physiological responses of fish early life stages to

338 hypoxia to identify the following candidate DEBkiss parameters to which to apply the hypoxia-

339 based correction factor: maximum assimilation rate, conversion efficiency of assimilates into

340 structure (growth), maximum somatic maintenance rate, embryo mortality rate, and post-hatch

341 mortality rate. Hypoxia effects on growth and hatching time can occur either through inhibition

342 of assimilation or through damage that reduces the conversion efficiency of assimilates to

343 growth. Hypoxia impact on survival may be caused directly through damage or by inhibition of

344 damage repair processes. Hypoxia impact on somatic maintenance rate may be most plausibly

345 represented as damage. We now discuss how these abstract concepts, damage and inhibition,

346 may relate to observations on hypoxia.

347 Assimilation is the transformation of food (or yolk) and oxygen into compounds that will

348 go to structure, maintenance, or reproduction (Kooijman, 2010a; Jager, 2018). Reduced food

349 consumption or reduced conversion of food into utilizable compounds, and thus limitation of

350 input of substrate to the SU, is a primary mechanism by which the fish energy budget is thought

351 to be impacted by hypoxia (Chabot and Dutil, 1999; Thomas et al., 2019 with findings

352 reinterpreted for DEBkiss).

353 Several genes controlling cell division and protein synthesis are regulated by hypoxia

354 (Ton et al., 2003), such as insulin-like growth factor binding protein 1 (IGFBP-1), a protein

355 controlled by hypoxia-inducible factor 1 (Hif-1) that has been shown to reduce growth and delay

356 development in fish embryos exposed to hypoxia (Kajimura et al., 2005; Kajimura et al., 2006;

357 Sun et al., 2011; Tian et al., 2014). This factor is thought to trade off growth for other oxygen-

358 demanding processes and help fish tolerate hypoxia. By preventing insulin-like growth factors

359 from binding to their receptors, IGFBP-1 inhibits signaling for cell division and differentiation

360 and energy can be diverted to processes necessary for survival (Kajimura et al., 2005). In the

361 DEBkiss model such forms of inhibition to the SU under hypoxia would be represented by

362 reduced assimilation rates, though the link to survival is not represented explicitly.

363 The conversion efficiency of assimilates to structure determines growth and hatch timing

364 because it represents the fraction of assimilates that are converted into structure rather than

365 burned on overhead costs of growth (Jager, 2018). When oxygen is low enough that anaerobic

366 metabolism must be used, this reduces conversion efficiency so that less growth results from the
367 same amount of yolk or food (Thomas et al., 2019). Damage to the SU may also be responsible
368 for reductions in conversion efficiency through lactate accumulation and consequential declines
369 in internal pH. Even at oxygen levels above the critical level at which oxygen consumption
370 declines, anaerobic glycolysis may increase (Nonnotte et al., 1993; Maxime et al., 2000; Wood et
371 al., 2018). Although capability for anaerobic glycolysis in embryos and yolk sac larvae appears
372 to vary widely across species (Wieser, 1995; Finn, 1995; Rombough, 1988), smaller fishes reach
373 harmful levels of anaerobic end-products much faster than larger fishes due to their higher mass-
374 specific metabolic rates (Nilsson and Östlund-Nilsson, 2008). We hypothesized that this
375 contributed to a smaller hatch size and slower growth post-hatch.

376 Maintenance in DEBkiss is the energy allocated to any processes that support the
377 integrity and functioning of the structural body (Jager, 2018), including homeostasis, damage
378 repair, and activity. Demand for more protein turnover and cell repair can increase the volume-
379 specific maintenance rate following damage (Bouma et al., 1994; Kooijman, 2010a) and indeed
380 maintenance has been shown to increase with damage to structural proteins (Maury et al., 2019).
381 In addition to damage repair, maintenance rate could be elevated by the activity required for
382 some of the behavioral responses fish exhibit under hypoxia (Thomas et al., 2019). *M. menidia*
383 exposed to hypoxia swim to the surface to use aquatic surface respiration, taking advantage of
384 the diffusion of oxygen from the air (Miller et al., 2016). This behavior is impossible in embryos
385 but has been observed in larvae (Cross et al., 2019). Fishes also expend energy on faster
386 ventilation and heartbeat when ambient DO is low to increase oxygen uptake (Kramer, 1987;
387 Maxime et al., 2000) and remove accumulated CO_2 and lactate (Perry et al., 2009; Heath and
388 Pritchard, 1965), but these capabilities may be limited until development has progressed further.

389 The maintenance flux in DEBkiss is represented in units of assimilated carbon required to
390 meet the energy demand from maintenance. It therefore is only indirectly related to respiration
391 rates measured as oxygen consumption. For example, an increase in the abstract maintenance
392 parameter in the model could be caused by an increase in anaerobic processes without impacting
393 oxygen consumption. The *measured* oxygen consumption rates of *M. menidia* early life stages
394 did not significantly increase under experimental chronic hypoxia, but great variability in
395 metabolic rates among individuals combined with the short respirometry periods used (<1 hour)

14

396   may make small increases related to damage repair or activity difficult to detect (Schwemmer et

397   al., 2020).

398   Although mortality is not a process directly represented by an SU, it could indirectly be

399   impacted by hypoxia effects on SUs through failure to meet developmental milestones –

400   particularly for hatching – or directly through increase in damage production or inhibition of

401   damage repair rates. In the parameter estimation using data from normoxic conditions (Section

402   2.3), our estimated survival parameter for embryo mortality was greater than that of larvae

403   (Table 1). If assimilation rate or conversion efficiency of *M. menidia* decreases under hypoxia,

404   the resulting slower egg buffer depletion would delay hatching, extending individuals' time in

405   the stage with greater mortality and thus accounting for reduced hatch survival under hypoxia.

406   We therefore hypothesized that if either assimilation rate or conversion efficiency is modified by

407   the hypoxia-based correction factor, additionally modifying the embryo mortality parameter

408   would consequently not be necessary to account for hypoxia effects on all four state variables.

409   However, this would not be the case for the post-hatch mortality parameter because none of the

410   processes in the DEBkiss model indirectly affect mortality after hatching, so changing either the

411   assimilation or conversion efficiency parameter in combination with the post-hatch mortality

412   parameter may be necessary to fully replicate the observed changes to growth, hatch timing, and

413   survival under hypoxia.

414

2.5. Hypoxia Effects

416   We tested the hypothesis that changes in *M. menidia* early life growth, hatch timing, and

417   survival under reduced oxygen (Cross et al., 2019) can be explained by inhibition or damage

418   linked to one or more DEBkiss processes (Figure 1). To summarize the experimental data on

419   static hypoxia effects we are attempting to explain by altering these parameters, the mean values

420   of data for each oxygen treatment are listed in Table 3. We used the parameter values from the

421   model fit to full life data and altered one or more parameters at a time with oxygen-dependent

422   correction factors, then fit the model to data for only the first 136 days by estimating a parameter

423   that controls the correction factor's relationship with DO. We only used early life data to fit the

424   hypoxia-altered parameters because we did not have late-life or reproductive data for multiple

425   oxygen treatments against which to validate observed changes. It did not make sense to include

426   later life data in the calculations of NLL that influence the parameter estimates or to speculate

15

427 about how well the predicted data match what we might expect to happen later in life if we not

428 only lack late-life hypoxia data but also do not expect full-life hypoxia to occur in nature.

429

Variable	7.7 mg L^{-1}	4.2 mg L^{-1}	3.1 mg L^{-1}	2.7 mg L^{-1}
Survival to hatching	74.3%	70.6%	85.8%	30.2%
Hatch time (egg buffer mass = 0)	6 days	7 days	8 days	9 days
Length at hatching	5.3 mm	4.6 mm	4.4 mm	4.1 mm
Larval length at 15 dph	15.8 mm	12.2 mm	9.2 mm	-
Larval survival to 15 dph	44.0%	22.2%	20.9%	0%

430 **Table 3. Summary of experimental data for each DO level.** The mean survival to hatching,

431 hatch time (at which egg buffer is zero), length at hatching, length at 15 dph, and survival to 15

432 dph from the different DO treatments in Cross et al. (2019). The control DO level means (7.7 mg

433 l^{-1}) also include data from Murray and Baumann (2018).

434

435   We derived a correction factor for *inhibition* using the framework developed by Muller et

436 al. (2019), in which inhibitors can act on SU dynamics in five different ways. Out of these,

437 *noncompetitive inhibition* is well-suited to this study because of the limitations of data

438 availability for *M. menidia*. In noncompetitive inhibition the arrival rate of substrate does not

439 affect the binding and dissociation of inhibitors and therefore requires little information about the

440 rate of food uptake (Muller et al., 2019). In this form of inhibition, the rate of assimilation by the

441 SU is:

442
$$J_A = f J_{Am}^a L^2 \left(\frac{1}{1 + \frac{j_i}{k_i}} \right) \tag{2}$$

443 where j_i is the arrival flux of the inhibitor and k_i is the dissociation parameter. The effect of this

444 relationship in our model is that assimilation declines as the arrival rate of hypoxia-related

445 inhibitors increases. We set j_i to depend on DO treatment above a DO threshold, DO$_c$, below

446 which j_i is infinitely large, which would bring the rate of the process it is inhibiting to zero:

447
$$j_i = \begin{cases} \infty & if\ DO \leq DO_c \\ \frac{1}{Z(DO - DO_c)} & if\ DO > DO_c \end{cases} \tag{3}$$

448 Z is a parameter that influences the shape of the relationship between j_i and DO. We defined the

449 correction factor c as the inhibition term (in parentheses in Equation 2) and replace j_i with the

450 function from Equation 3 for DO > DO$_c$ to derive the correction factor c:

451 $$c = \frac{1}{1 + \frac{1}{k_i Z (DO - DO_c)}}$$ (4)

452 As only the product of the parameters k_i and Z appear in the formula and we have no need to

453 estimate them separately, they can be combined into one parameter as Z. Simplifying Equation 4

454 and adding in the case for which $DO \leq DO_c$ gives us the following correction factor:

455 $$c = \begin{cases} 0 & if\ DO \leq DO_c \\ \frac{Z(DO-DO_c)}{1+Z(DO-DO_c)} & if\ DO > DO_c \end{cases}$$ (5)

456 The relationship between c and DO for three different sample values of Z, the parameter

457 to be estimated, is shown in Figure 2. A larger Z value keeps c higher as oxygen decreases before

458 a more abrupt drop, while a smaller Z gives a more constant decline in c with hypoxia. The value

459 of c cannot exceed 1. DO_c was fixed at a biologically relevant level of 2.04 mg L^{-1}, which is the

460 critical oxygen level below which embryonic routine metabolism becomes highly oxygen-

461 dependent (Schwemmer, 2023). Attempts to estimate DO_c and Z simultaneously showed that

462 leaving DO_c free did not improve the ability of the correction factor to fit the hypoxia data.

463

464
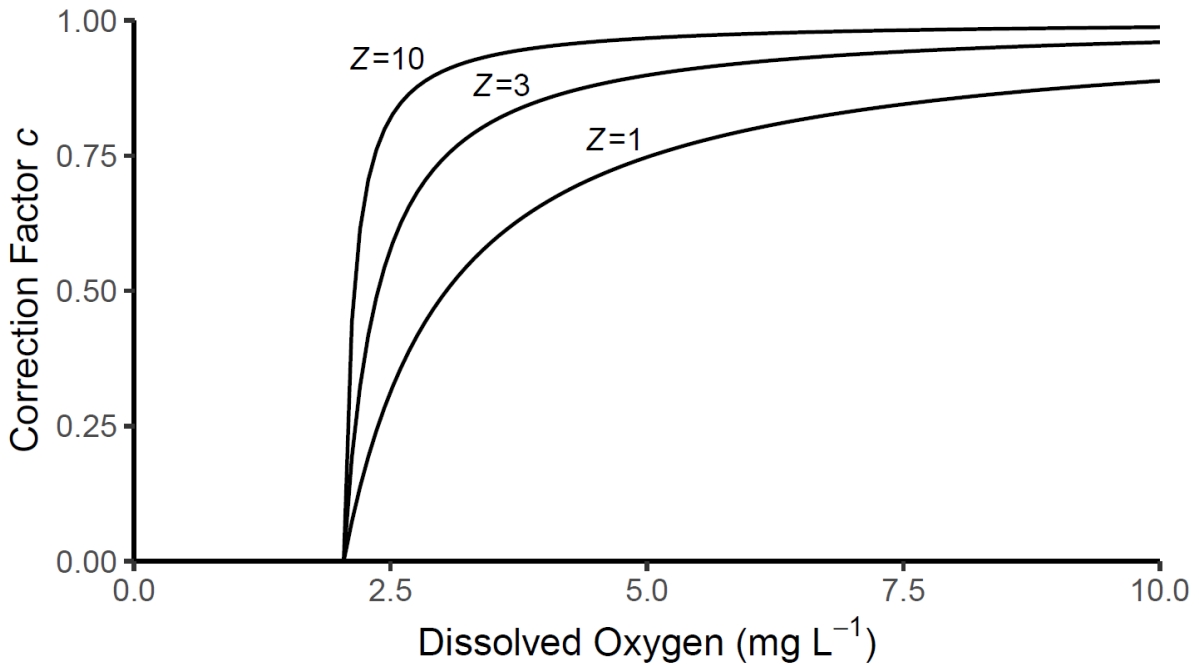
465 **Figure 2. The correction factor c used to apply hypoxia effects to DEBkiss parameters.** The

466 effect of DO on correction factor c is shown at three different values of the exponential

17

467   parameter Z. Actual estimated Z values are listed in Table 4, and the three Z values used in this

468   figure are sample values to show how Z affects the relationship between DO and c.

469

470   Similar simplification of the reasoning by Muller et al. (2019) can be used to derive an

471   analogous correction factor for *damage*. Assuming that the proportional change in the rate of

472   damage production to the SU (e.g. via "damage inducing compounds"; Kooijman 2010a)), j_d has

473   the same form as Equation (3). If damage production is quickly balanced by repair or mitigation,

474   then fluxes that decrease through hypoxia will again be reduced by the factor given by Equation

475   (5). This was recognized by Muller et al. (2019) who noted that if damage production is much

476   slower than the maximum production rate of an SU, the formalism for noncompetitive damage is

477   equivalent to that of noncompetitive inhibition (Muller et al., 2019). Further submodels relating

478   damage to rates that may increase in response to hypoxia (e.g. maintenance and mortality) are

479   needed to derive functional forms for appropriate conversion factors here. Absent information to

480   support such submodels, we hypothesize that the increase was inversely proportional to c defined

481   by Equation (5).

482   The correction factor c was multiplied by J^a_{Am} and y_{VA} because these parameters were

483   hypothesized to decrease under hypoxia irrespective of the underlying cause (inhibition or

484   damage). Reductions in the parameter y_{VA} through hypoxia are most plausibly interpreted as

485   damage, the irreversible destruction of functionality of an SU. However, the parameters for

486   maintenance and mortality were divided by c because they were hypothesized to increase, rather

487   than decrease, with damage production and inhibition.

488   To find the best value of Z for each DEBkiss parameter or combination of parameters, we

489   added Z as a model parameter and estimated it using the BYOM optimization to minimize NLL.

490   We weighted the data equally across treatments to correct for differences in sample size across

491   treatments and prevent one treatment group from disproportionately affecting the estimation of

492   Z, so that all weights within each treatment added up to the same number. We did not apply the

493   correction factor to J^a_{Am} and y_{VA} simultaneously because they are multiplied together to obtain J_V

494   and their individual contributions to the growth and egg buffer depletion cannot be fully

495   separated. We only compared the fit of models in which c was applied to parameter(s) that

496   resulted in all three early life datasets – total length, egg buffer mass, and survival – being

497 affected by hypoxia. As a result, either J^a_{Am} or y_{VA} is in each candidate model, because J^v_M, μ_{emb},

498 and μ_{lar} do not affect egg buffer depletion.

499   To identify the most likely version of the model (which parameter or combination of

500 parameters best explains the hypoxia effects on the state variables), we estimated Z for each of

501 these scenarios and calculated Akaike's Information Criterion for small sample sizes (AICc). We

502 compared the AICc between each model using the difference between AICc values (ΔAICc) and

503 the relative likelihood of each model using Akaike weights:

$$w_i(AICc) = e^{-0.5 \cdot \Delta_i AICc} / \sum_{k=1}^{K} e^{-0.5 \cdot \Delta_k AICc}, \qquad (6)$$

505 where w_i(AICc) is the Akaike weight of each model i, Δ_iAICc is the difference between each

506 model i and the model with the lowest AICc (AICc$_{min}$), and the denominator calculates the sum

507 of relative likelihoods for every model starting at the first model k (Wagenmakers and Farrell,

508 2004). We used ΔAICc and ratios of Akaike weights to determine which combination of

509 parameters best fit the data when inhibition or damage was applied and, therefore, which DEB

510 processes best explain the hypoxia effects observed in experiments (Table 4).

511

3. Results

3.1. DEBkiss Model

514   We obtained realistic fits to the full life cycle data (Figure 3). The only exception is late-

515 life survival, for which the mortality was too high beyond the larval stage but could not be better

516 fit due to lack of full-life survival data (Figure 3D). Silversides are an annual species so survival

517 should be greater than 0% after 150 days. However, this did not impair our ability to model the

518 effects of hypoxia on early life survival, which is most important given that the present study

519 focuses on hypoxia in the early life stages. Estimating y_{VA} returned a value much lower than 0.8,

520 which is the value suggested by Jager (2018) and has been applied in DEBkiss models of other

521 species (e.g. Jager et al., 2018; Hamda et al., 2019). However, our value of $y_{VA} = 0.365$ is close to

522 the maximum growth efficiency of 0.375 measured in the closely related *M. beryllina* (Letcher

523 and Bengtson, 1993). This gave a realistic fit to the length data and allowed a detailed and very

524 close fit to egg buffer mass over time (hatch timing). The observed and predicted data for full life

525 span are plotted in Figure 3.
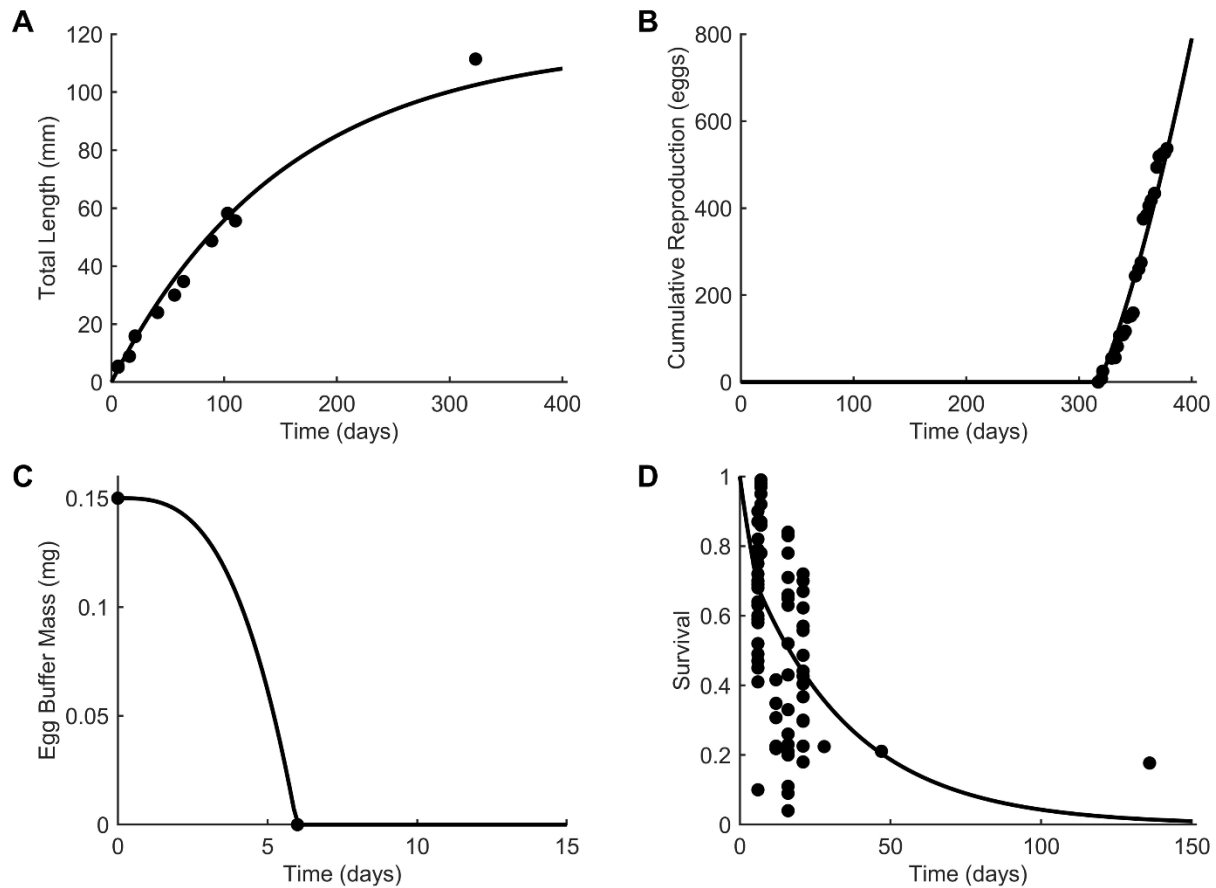
Figure 3. Full life model fits to data for four state variables. Predicted (lines) and observed data (dots) for the DEBkiss model of *M. menidia* are shown. The state variables are (A) total length (mm) over time (days), (B) cumulative reproduction (eggs) over time (days), (C) egg buffer mass (mg) over time (days), and (D) survival over time (days). Predicted data lines were calculated with the parameter values listed in Table 1.

3.2. Hypoxia Effects

      Applying the oxygen-dependent correction factor to the parameter combinations listed in Table 4 reproduced the direction of experimentally observed hypoxia effects, e.g. increasing J^a_{Am} reduced total length, increased time until egg buffer mass reaches 0, and reduced survival. The best model of experimental hypoxia effects on *M. menidia* early life stages simultaneously had y_{VA} multiplied by c, and μ_{emb} and μ_{lar} divided by c (Figure 4, Table 4, Figure S1). Although

20

541 applying damage to y_{VA} alone affected all three state variables, concurrently increasing both

542 mortality parameters improved the fit to the data (Table 4). The model in which the correction

543 factor was applied to y_{VA}, μ_{emb}, and μ_{lar} also had the lowest AICc of all candidate models, with an

544 AICc of 794.03 (AICc$_{min}$). Adding a correction factor to J^v_M in simultaneously with these three

545 parameters yielded a slightly higher AICc of 795.97 (Table 4). The ratio of Akaike weights

546 shows that the model with c applied to y_{VA}, μ_{emb}, and μ_{lar}, is 2.67 times as likely as the one with c

547 concurrently applied to J^v_M (Table 4). Applying a damage effect to maintenance was therefore

548 not considered to have improved the fit. After estimating Z we calculated the values of y_{VA}, μ_{emb},

549 and μ_{lar} when their respective correction factors are applied for each DO level (Table 5).

550

551

Parameter(s) affected by hypoxia correction factor	Estimated Z [95% CI]	AICc	ΔAICc	Akaike weight
J^a_{Am}	3.019 [2.512-3.612]	856.06	62.03	2.5e-14
y_{VA}	1.818 [1.601-2.342]	848.65	54.62	1.0e-12
$J^a_{Am} + J^v_M$	3.105 [2.651-3.726]	855.00	60.97	4.2e-14
$y_{VA} + J^v_M$	1.985 [1.688-2.774]	850.64	56.61	3.7e-13
$J^a_{Am} + \mu_{emb}$	2.804 [1.605-3.287]	823.24	29.21	3.3e-7
$y_{VA} + \mu_{emb}$	1.801 [1.570-2.167]	808.12	14.09	6.3e-4
$J^a_{Am} + \mu_{lar}$	2.930 [2.165-3.428]	838.17	44.14	1.9e-10
$y_{VA} + \mu_{lar}$	1.767 [1.536-2.111]	821.30	27.27	8.7e-7
$J^a_{Am} + \mu_{emb} + \mu_{lar}$	2.819 [1.920-3.286]	810.21	16.18	2.2e-4
$y_{VA} + \mu_{emb} + \mu_{lar}$	**1.827 [1.620-2.269]**	**794.03**	**0**	**0.72**
$J^a_{Am} + J^v_M + \mu_{emb} + \mu_{lar}$	2.913 [2.288, 3.387]	809.96	15.93	2.5e-4
$y_{VA} + J^v_M + \mu_{emb} + \mu_{lar}$	1.981 [1.700, 2.456]	795.97	1.94	0.27

552 **Table 4. Parameter Z estimates and model selection results.** The estimated Z value, AICc,

553 ΔAICc, and Akaike weights when the correction factors were applied to each parameter or

554 combination of parameters. ΔAICc and Akaike weights were calculated with AICc$_{min}$ = 794.03

555 for the $y_{VA} + \mu_{emb} + \mu_{lar}$ model (bold).

556

557
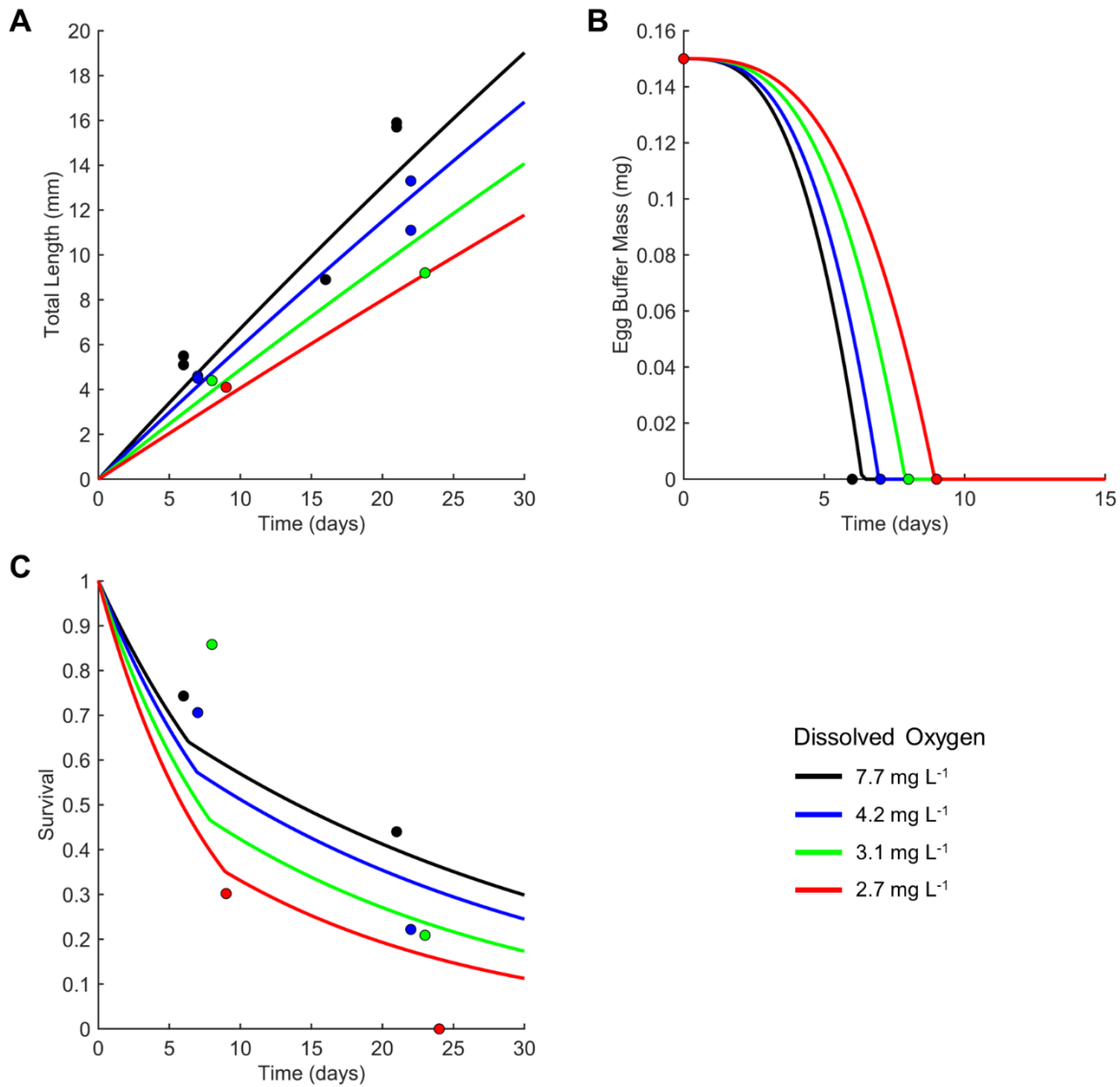
558
559
560 **Figure 4. Best fit of DEBkiss model to experimental data from four DO levels**. The best fit of

561 the predicted data (lines) to the observed data (dots) for four DO levels is shown, for early life

562 data only. The best fitting model was selected based on lowest AICc. (A) is total length (mm)

563 over time (days), (B) is egg buffer mass (mg) over time (days), and (C) is survival over time

564 (days), with means rather than all data plotted for survival for ease of viewing. Full datasets used

565 to estimate the correction factor parameter Z are plotted in Figure S1.

566

567 Interestingly, although J^a_{Am} affects the variables similarly to y_{VA}, the ratio of Akaike

568 weights showed that the best fitting model is about 3000 times as likely as the version applying

569 inhibition to J^a_{Am}, μ_{emb}, and μ_{lar} (Table 4). Reducing J^a_{Am} with hypoxia using the correction factor

570 resulted in a visually good fit to the data across oxygen levels and variables. Simultaneously

571 applying c to J^a_{Am} and both mortality parameters improved the fit compared to only applying it to

572 J^a_{Am}, but this model fit less well than the version that applied c to y_{VA}, μ_{emb}, and μ_{lar}, with an AIC

573 value of 810.21 in the former model compared to 794.03 in the latter.

574 The estimated best value of Z, the exponential coefficient in the correction factor c,

575 enables us to calculate that y_{VA} at the lowest oxygen level is 55% of its value with no hypoxia

576 stress. Reducing conversion efficiency alone produced small differences in survival at hatching

577 because it prolongs the time spent in the embryo stage, which has a greater mortality rate than

578 post-hatching in our model. Dividing both the pre- and post-hatching mortality rates by c more

579 closely predicted the reduced survival rates in the low DO treatments, resulting in a best fitting

580 model that explained observed hypoxia effects well by altering conversion efficiency, embryo

581 mortality, and post-hatch mortality.

582

	Product of correction factor and initial parameter value			
	7.7 mg L^{-1}	4.2 mg L^{-1}	3.1 mg L^{-1}	2.7 mg L^{-1}
y_{VA}	0.333 [0.329, 0.339]	0.291 [0.284, 0.303]	0.240 [0.230, 0.257]	0.199 [0.188, 0.218]
μ_{emb}	0.0701 [0.0689, 0.0709]	0.0801 [0.0770, 0.0822]	0.0970 [0.0906, 0.101]	0.117 [0.107, 0.124]
μ_{lar}	0.0322 [0.0317, 0.0326]	0.0369 [0.0354, 0.0378]	0.0446 [0.0417, 0.0466]	0.0539 [0.0492, 0.0571]

583 **Table 5. Effects of correction factor c on parameters.** The value of the DEBkiss parameters

584 that best reproduce the hypoxia effects observed experimentally, calculated (with 95%

585 confidence intervals in brackets) for each DO treatment level using the correction factor c and

586 the estimated value of $Z = 1.827$.

587

588

589 **4. Discussion**

590 By combining experimental data with unified principles for energetic allocation that are

591 broadly applicable across species, we identified the conversion efficiency of assimilates into

592 structure as the most likely process by which low oxygen levels affect early life stages of *M.*

593 *menidia*. In comparing combinations of DEBkiss parameters that influence the ecological

594 endpoints (total length, hatch timing, and survival), we discovered that applying correction

23

595   factors based on damage production to the growth SU to reduce conversion efficiency (y_{VA}) and

596   increase pre- and post-hatching mortality rates (μ_{emb} and μ_{lar}) best predicted the experimental

597   effects of hypoxia on larval length, time to hatching, and early life survival. Through this model

598   we have found evidence that the mechanism largely responsible for the observed hypoxia

599   impacts on growth, hatch timing, and survival is the efficiency with which assimilated food or

600   egg yolk is converted into structure. The limitations of this inference are discussed later.

601   Changes to assimilation in response to hypoxia have been recorded in other species, but

602   the direction of that effect is species-dependent (reviewed in Thomas et al., 2019). In *M.*

603   *menidia*, however, reducing assimilation with hypoxia rather than conversion efficiency yielded

604   a worse fit despite the two parameters' similar contributions to the DEBkiss model in that both

605   parameters are used to calculate predicted growth and egg buffer depletion. In our

606   implementation of hypoxia effects on SUs, these two parameters are assumed to be impacted by

607   different molecular mechanisms but the same noncompetitive inhibition-based correction factor,

608   due to the assumption that the maximum rate at which the SUs form product is much greater than

609   the damage production rate (Muller et al., 2019). Reducing either assimilation or conversion

610   efficiency would extend developmental time, which is consistent with previous work showing

611   yolk absorption slows under hypoxia (Polymeropoulos et al., 2017). As maintenance costs must

612   continue to be paid, this would increase the energy expended to produce each unit of structure

613   (Kamler, 2008). However, the mechanism for reduced conversion efficiency is most plausibly

614   interpreted as damage to the synthesizing unit, perhaps from buildup of anaerobic byproducts,

615   and repairing the SU incurs additional maintenance costs compared to inhibition which requires

616   no repair (Bouma et al., 1994; Kooijman, 2010a; Muller et al., 2019). Conversion efficiency can

617   also be reduced by the far less efficient production of ATP through anaerobic respiration

618   combined with slower rates of tissue differentiation. The experimental DO levels are greater than

619   the critical oxygen levels for oxygen-independent routine metabolism (P_{crit}) of 2.04 mg L^{-1} and

620   1.56 mg L^{-1} for embryos and 5dph larvae, respectively (Schwemmer, 2023). P_{crit} has been

621   assumed by some to be the oxygen level at which anaerobic metabolism is triggered, but there is

622   abundant evidence that some level of anaerobic metabolism can occur well above P_{crit} (Nonnotte

623   et al., 1993; Maxime et al., 2000; Wood et al., 2018). Additional activity such as swimming

624   bursts can drive up the need for anaerobiosis (Di Santo et al., 2017). Our evidence that

625   conversion efficiency is reduced by hypoxia-induced damage suggests that anaerobic metabolism

626   may be a mechanism of hypoxia effects in *M. menidia* early life stages even at oxygen levels

627   above P_{crit}.

628   While y_{VA} is the best parameter to explain the hypoxia effects according to our model and

629   AICc, it is nonetheless possible that J^a_{Am} is responsible for an unknown portion of the hypoxia

630   effects. Because of near collinearity between J^a_{Am} and y_{VA}, our model does not allow us to test for

631   the possibility that both parameters are simultaneously contributing to the observed hypoxia

632   effects. It is not possible to simultaneously estimate both parameters as their product is used to

633   calculate growth in the model; we can adjust one or the other with the correction factor and get

634   similar effects on the flux for growth with no way of determining which is correct. We therefore

635   cannot test for partial contribution of the two parameters to hypoxia effects or quantify their

636   relative contributions. If conversion efficiency were the only parameter varying across hypoxia

637   treatments, one might expect the offspring to fully deplete the egg buffer and hatch at the same

638   time, but with hatch size increasing with DO level. However, adjusting conversion efficiency

639   with hypoxia does account for the observed significant differences in hatch timing between DO

640   treatments in *M. menidia* larvae (Cross et al., 2019) because y_{VA} reduces the body size at a given

641   time, indirectly reducing the assimilation flux due to smaller body volume.

642   Although both conversion efficiency and assimilation can explain hypoxia effects on total

643   length and egg buffer mass over time, reducing them only produced a small decrease in survival

644   relative to the data. Simultaneously applying c to both mortality rates better captured the great

645   reductions in survival at both hatching and 15 dph with hypoxia. In the experiments, the lowest

646   oxygen level (2.7 mg L^{-1}) had a mean hatch survival of 30.2% while the mean survival in the

647   other three treatments was over 70% (Cross et al., 2019). By 15 dph fish from all three low

648   oxygen treatments had lower survival than those from the normoxic treatment (Cross et al., 2019;

649   Table 3). Including hypoxia effects for both pre- and post-hatching mortality rates allowed the

650   model to predict these stage-specific differences in hypoxia effects more closely and improve the

651   fit based on ΔAICc (Table 4). The additional mortality that was not accounted for by y_{VA} may

652   have been related to unrepaired damage from buildup of toxic compounds during anaerobic

653   metabolism (Richards, 2011). The mortality could also have resulted from failing to meet

654   energetic demands with either aerobic or anaerobic metabolism (Richards, 2009) and,

655   specifically in embryos, failure to reach a viable level of complexity before the yolk is depleted

656   (Jager et al., 2013). Measurement of anaerobic byproducts such as lactate and morphometric

25

657 assessment of dead embryos and larvae could help to identify the mechanisms underlying the

658 mortality rates in future work. Although survival does not approach 0% during the larval stage in

659 our best fitting model (Figure 4), all experimental replicates of the 2.7 mg L^{-1} DO treatment had

660 0% survival by 15 dph, making larvae apparently more sensitive than embryos (Cross et al.,

661 2019). The authors of the study attribute this to a possibly lower ability to suppress metabolism

662 in larvae compared to embryos. While the increased mobility of larvae may allow aquatic surface

663 respiration (Miller et al., 2016; Cross et al., 2019) and escape from hypoxia in a patchy and

664 stratified estuarine environment, activity comes with elevated maintenance costs in addition to

665 those required to begin feeding almost immediately after hatching (Middaugh and Lempesis,

666 1976). This may also be a crucial time to repair damage to the SU (Muller et al., 2019), and the

667 combination of these additional maintenance demands may be too great to meet without

668 restoration of normoxia. Though beyond the scope of this work, a model that captures stage-

669 specific differences in maintenance costs and links them explicitly to survival may better capture

670 the mechanism of high mortality in larvae.

671   Adding a correction factor to the volume-specific maintenance rate in addition to y_{VA},

672 μ_{emb}, and μ_{lar} did not substantially improve the fit according to AICc, suggesting that increasing

673 maintenance costs is not an important bioenergetic mechanism underlying hypoxia response in

674 early life stages. This is consistent with laboratory measurements showing no effect of these

675 hypoxia levels on embryonic or larval metabolic rates (Schwemmer et al., 2020), but as noted

676 earlier interpretation of respiration data is challenging and there was high individual variability

677 in the data. In our model, egg buffer depletion is insensitive to changes in volume-specific

678 maintenance costs, requiring a quadrupling to see a noticeable delay in hatching. Changing

679 maintenance has much greater effects on length later in life while failing to explain differences in

680 length at the time of hatching. Repairing damage and increasing ventilation and swimming

681 activity could both increase maintenance costs (Thomas et al., 2019), but at the embryo stage

682 very little activity is possible. A common response to hypoxia in some fish embryos is premature

683 hatching (Kamler, 2008) which could allow swimming escape responses that increase

684 maintenance costs and in theory reduce growth, but studies on chorion removal have shown that

685 the increased mobility can improve growth despite hypoxia exposure (Ciuhandu et al., 2005;

686 Ninness et al., 2006). Some studies on fish responses to hypoxia suggest maintenance may drop

687 temporarily due to the reduced capacity for aerobic metabolism at low DO levels, then

26

688   subsequently be temporarily elevated after oxygen is restored because of recovery demands such

689   as paying oxygen debt and removing or repairing damage from anaerobic byproducts (Heath and

690   Pritchard, 1965; Claireaux and Chabot, 2016; Thomas et al., 2019). Such fluctuations in

691   maintenance were not discernible in the time scale of our model, but future work should attempt

692   to model the *M. menidia* early life energy budget during recovery from hypoxia.

693   Understanding the mechanisms of reduced growth and survival under hypoxia through

694   DEB theory is useful for predicting life history effects, and although modeling population growth

695   rates was not within the scope of this study, our results have implications for processes that

696   influence fish population dynamics. The predicted data resulting from fitting to early life data

697   with a hypoxia-based correction factor predicts reductions in long-term growth and survival that

698   would certainly be detrimental to population growth under extended periods of low oxygen.

699   Under this model, even restoring normoxia after 15 days would result in smaller size at age and

700   survival rates than the control group, and damage to the SU is not reversed upon return to

701   normoxia, but rather requires energy to repair (Muller et al., 2019). However, compensation of

702   growth may be possible in aquatic ectotherms after exposure to hypoxia (Wei et al., 2008) and

703   other stressors (Russell and Wootton, 1992; Nicieza and Metcalfe, 1997; Ali et al., 2003).

704   Delayed hatching and slower growth can lead to enhanced vulnerability to predation (Chambers

705   and Leggett, 1987; Takasuka et al., 2007), further reducing fish survival rates beyond those

706   observed in controlled laboratory conditions, although this is not always the case (Lankford et

707   al., 2001; Robert et al., 2023). An important assumption of our model is that several of the

708   parameters have the same value across life stages (e.g. J^a_{Am}, J^v_M, y_{VA}) and similarly that values of

709   the hypoxia correction factors are the same regardless of life stage. We lacked data on the effects

710   of hypoxia on the proportion of total energy allocated to reproduction (1-κ), which is an

711   additional component of DEB useful in connecting organismal effects to populations. Future

712   experimentation could provide the adult-stage information that is needed to extend this DEB

713   model to predict population growth, which would be useful for resource management

714   applications (Kooijman et al., 2020; Lavaud et al., 2021), given the ecological importance of

715   forage fishes and the value of model species like *M. menidia*.

716   The oxygen levels in the estuaries inhabited by *M. menidia* undergo great diel and

717   seasonal fluctuations (Baumann et al., 2015). The effects of fluctuating DO cannot be resolved in

718   the time scales used by our DEBkiss model, so we assumed constant DO levels. As a result, the

719   model is more useful in identifying mechanisms than in quantitatively predicting how *M.*

720   *menidia* will respond to realistic hypoxia scenarios, as lifelong constant hypoxia is unrealistic

721   and this assumption may lead to overestimation of hypoxia effects. Studies comparing fish

722   responses to static and fluctuating hypoxia treatments have suggested that fluctuations provided

723   temporary relief and reduced sensitivity (Cross et al., 2019; Williams et al., 2019; Wang et al.,

724   2021), although conflicting results also exist (Morrell and Gobler, 2020). It is also unrealistic for

725   only a single environmental factor, in this case hypoxia, to influence the energy budget. Other

726   studies have applied correction factors to DEB parameters to model other species' responses to

727   hypoxia (Lavaud et al., 2019; Aguirre-Velarde et al., 2019), seawater acidification (Jager et al.,

728   2016; Moreira et al., 2022; Pousse et al., 2022) and pollutants (Muller et al., 2010; Desforges et

729   al., 2017). The success of this approach with a wide variety of stressors makes it an ideal

730   supplement to multistressor experiments, which are limited by logistical constraints. Modeling

731   stressor effects with DEBkiss parameters can yield additional information about energetic

732   mechanisms of responses and, with careful attention to the assumptions being made, may be

733   useful in extrapolating stressor effects to additional magnitudes or combinations of stressors that

734   would have been impractical to test experimentally, or to species with certain shared physiology

735   or life history traits (Goussen et al., 2020; Boult and Evans, 2021). In the case of *M. menidia*,

736   previous work showed that high CO_2 increases oxygen dependence of metabolism under both

737   chronic (Schwemmer et al., 2020) and acute hypoxia (Schwemmer, 2023). Adding oxygen as a

738   second substrate in the SU would allow a DEB model to incorporate the oxygen limitation that is

739   evidently induced by acidification.

740   Our best fitting model overestimated time to hatching at 7.7 mg L^{-1} DO and

741   overestimated survival at age for the 2.7 and 4.2 mg L^{-1} treatments, which suggests there either

742   may be a different nonlinear correction factor function that better fits the relationship between

743   DO and the DEBkiss parameters or that there were additional factors contributing to these

744   differences that the model does not account for. For example, we do not have data on gonad

745   development or reproductive output later in life after rearing *M. menidia* in hypoxia, which

746   would allow us investigate if κ is an affected parameter. Hypoxia can reduce gonadosomatic

747   index and gonad development in fish, suggesting that the reproductive branch of the energy

748   budget might require additional energy to be redirected from the somatic branch (Wu et al.,

749   2002; Thomas et al., 2006; Landry et al., 2007). Despite the potential for improvements with

28

750 more data, the model was able to replicate the direction of effects and even account for some

751 hypoxia effects in all three state variables simultaneously by changing only one parameter, either

752 conversion efficiency or assimilation. Further, it provided these reasonable fits using an SU

753 model based in well-studied and widely applicable Michaelis-Menten-Briggs-Haldane enzyme

754 kinetics (Muller et al., 2019) rather than a more specialized or complex correction factor.

755   We end with a comment on the limitation of the "DEBtox" approach (Kooijman et al.,

756 2009), a toxicology application of DEB from which DEBkiss stems, to identifying physiological

757 modes of action in response to environmental stress. In Section 1 we cite the paper by Romoli et

758 al. (2024) that highlighted the difficult modeling choices that are required. Here we chose to use

759 DEBkiss coupled with several hypothesized responses to hypoxia. We selected the combination

760 of DEB model and response hypothesis that best described given data (in an information

761 theoretic sense using AICc), *conditional on the "correctness" of the model and of assumed*

762 *values for some parameters*. Yet, for a case study in ecotoxicology, Romoli et al. showed that a

763 different dominant physiological model of action was selected when using two different

764 underlying DEB models that both give visually good fits to control data. Muller et al. (2010)

765 demonstrated a related issue for a study of early life stage growth by identifying best fit

766 submodel for larval growth of two closely related bivalve species exposed to mercury.

767 Implausibly, the selected submodels were different to the extent that the best fit for one species

768 was the worst for the other.

769   In the preceding discussion, we have offered a few suggestions for empirical work on

770 whole organisms that would significantly help narrow down the DEB processes responsible for

771 responses to hypoxia. However, it is likely that an additional, very promising way forward is to

772 determine *suborganismal* processes co-occurring with the observed whole-organism responses.

773 Transcriptomic data represent a particularly promising candidate (Murphy et al 2018). We

774 recognized this qualitatively in Section 2.4 when invoking genes controlling cell division and

775 protein synthesis that are regulated by hypoxia-inducible factors. Stevenson et al. (2023)

776 demonstrated the power of transcriptomic data in a study of killifish embryos exposed to a

777 toxicant. The molecular data helped to identify damage mechanisms that in turn led to changes in

778 DEB parameters. There are many further exciting possibilities for integrating suborganismal

779 (molecular) data with DEBtox modeling.

780

29

5. Conclusions

With this simple and widely applicable DEBkiss model we were able to attribute hypoxia-related variability in *M. menidia* growth, hatch timing, and survival to damage-induced reductions in conversion efficiency of assimilates into structure. Applying hypoxia corrections simultaneously to conversion efficiency and the mortality parameters for embryos and larvae provided the best fit, suggesting that hypoxia leads to both wasted energy and damage that cannot be sufficiently repaired in the early life stages. As lifelong, constant oxygen conditions are unrealistic in nature, the patterns modeled in this study should not be interpreted as a standalone prediction of what will happen to wild *M. menidia* populations as coastal hypoxia intensifies. Instead, this approach demonstrates the value of identifying energetic processes responsible for whole-organism effects of hypoxia to understand underlying energetic processes that are often time, labor, and cost-intensive to measure empirically, particularly in the early life stages, when biomass available for sampling is small and developmental changes are rapid. Through doing so we were able to support the utility of modeling inhibition and damage to synthesizing units and highlight conversion efficiency of food into growth as a primary mechanism by which hypoxia impacts an ecologically important forage fish and model species. Measuring suborganismal processes to identify physiological modes of action can refine this model so that it can better model this species' response to realistic hypoxia scenarios and, ultimately, how reductions in conversion efficiency could affect energy flow through food webs.

Declaration of Competing Interest

The authors do not declare any competing interests.

Author Contributions

817

Data and Code

823 The datasets used for modeling can be found on BCO-DMO: early life total length, survival, and

824 hatching: doi: 10.1575/1912/bco-dmo.742200; early life total length with oxygen treatments: doi:

825 10.1575/1912/bco-dmo.777130.1; hatching and survival with oxygen treatments: doi:

826 10.1575/1912/bco-dmo.777117.1; total length of adults: doi: 10.26008/1912/bco-dmo.845906.1;

827 total length of larvae and juveniles: doi: 10.1575/1912/bco-dmo.652124; egg production: doi:

828 10.26008/1912/bco-dmo.845633.1. The BYOM and DEBkiss packages can be found at

829 https://www.debtox.info/byom.html. The code for inputting data, parameter estimation, and

830 plotting, for both the normoxic model and the model with hypoxia effects, can be found at

831 github.com/tschwemmer/MenidiaDEB.

832

References

Aguirre-Velarde, A., Pecquerie, L., Frederic, J., Gerard, T., and Flye-Sainte-Marie, J. 2019. Predicting the energy budget of the scallop *Argopecten purpuratus* in an oxygen-limiting environment. *J. Sea Res.*, 143: 254-261. https://doi.org/10.1016/j.seares.2018.09.011

Ali, M., Nicieza, A., and Wootton, R. J. 2003. Compensatory growth in fishes: a response to growth depression. *Fish and Fisheries*, 4: 147-190. https://doi.org/10.1046/j.1467-2979.2003.00120.x

AmP. 2021. Online database of DEB parameters, implied properties and referenced underlying data. www.bio.vu.nl/thb/deb/deblab/add_my_pet/ (data accessed: March 3, 2023).

AmPtool, 2022. Software package, https://github.com/add-my-pet/AmPtool/

Baumann, H. 2019. Experimental assessments of marine species sensitivities to ocean acidification and co-stressors: how far have we come? *Can. J. Zool.*, 97: 399-408. dx.doi.org/10.1139/cjz-2018-0198

Baumann, H. and Smith, E. M. 2018. Quantifying Metabolically Driven pH and Oxygen Fluctuations in US Nearshore Habitats at Diel to Interannual Time Scales. *Estuaries and Coasts*, 41: 1102-1117. https://doi.org/10.1007/s12237-017-0321-3

[dataset] Baumann, H., Nye, J. (2016) Laboratory study of long-term growth in juvenile *Menidia menidia* (Atlantic silverside) at contrasting CO_2 levels for 16 to 122 days in 2015. Biological and Chemical Oceanography Data Management Office (BCO-DMO). (Version final) Version Date 2016-07-07. doi:10.1575/1912/bco-dmo.652124 [accessed 2022-03-30]

[dataset] Baumann, H., Cross, E. (2019) Growth data from static and fluctuating pCO_2 x dissolved oxygen (DO) experiments on *Menidia menidia*. Biological and Chemical Oceanography Data Management Office (BCO-DMO). (Version 1) Version Date 2019-09-20. doi:10.1575/1912/bco-dmo.777130.1 [accessed 2022-03-30]

[dataset] Baumann, H., Cross, E. (2019) Survival data from static and fluctuating pCO_2 x dissolved oxygen (DO) experiments on *Menidia menidia*. Biological and Chemical Oceanography Data Management Office (BCO-DMO). (Version 1) Version Date 2019-09-20. doi:10.1575/1912/bco-dmo.777117.1 [accessed 2022-03-30]

[dataset] Baumann, H., Nye, J. (2021) Data from the spawning trial in a study of CO_2 and temperature-specific reproductive traits in *Menidia menidia*. Biological and Chemical Oceanography Data Management Office (BCO-DMO). (Version 1) Version Date 2021-04-23. doi:10.26008/1912/bco-dmo.845633.1 [accessed 2022-03-30]

[dataset] Baumann, H., Nye, J. (2021) Data from the fecundity trial in a study of CO_2 and temperature-specific reproductive traits in *Menidia menidia*. Biological and Chemical

879   Oceanography Data Management Office (BCO-DMO). (Version 1) Version Date 2021-
880   03-18. doi:10.26008/1912/bco-dmo.845906.1 [accessed 2022-03-30]
881

882 Baumann, H., Wallace, R. B., Tagliaferri, T., and Gobler, C. J. 2015. Large Natural pH, CO_2 and
883   O_2 Fluctuations in a Temperate Tidal Salt Marsh on Diel, Seasonal, and Interannual Time
884   Scales. *Estuaries Coasts*, 38: 220-231. doi: 10.1007/s12237-014-9800-y
885

886 Bengtson, D. A. 1984. Resource partitioning by *Menidia menidia* and *Menidia beryllina*
887   (Osteichthyes: Atherinidae). *Mar. Ecol. Prog. Ser.*, 18: 21-30.
888

889 Bianchini, K. and Wright, P. A. 2013. Hypoxia delays hematopoiesis: retention of embryonic
890   hemoglobin and erythrocytes in larval rainbow trout, *Oncorhynchus mykiss*, during
891   chronic hypoxia exposure. *J. Exp. Biol.*, 216(23): 4415-4425.
892   https://doi.org/10.1242/jeb.083337
893

894 Boult, V. L. and Evans, L. C. 2021. Mechanisms matter: Predicting the ecological impacts of
895   global change. *Glob. Change Biol.*, 27(9): 1689-1691. https://doi.org/10.1111/gcb.15527
896

897 Bouma, T. J., De Visser, R., Janssen, J. H. J. A., De Kock, M. J., Van Leeuwen, P. H., and
898   Lambers, H. 1994. Respiratory energy requirements and rate of protein turnover in vivo
899   determined by the use of an inhibitor of protein synthesis and a probe to assess its effect.
900   *Physiol. Plant.*, 92: 585-594. https://doi.org/10.1111/j.1399-3054.1994.tb03027.x
901

902 Brandt, S. B., Gerken, M., Hartman, K. J., and Demers, E. 2009. Effects of hypoxia on food
903   consumption and growth of juvenile striped bass (*Morone saxatilis*). *J. Exp. Mar. Biol.*
904   *Ecol.*, 381: S143-S149. doi: 10.1016/j.jembe.2009.07.028
905

906 Breitburg, D., Levin, L. A., Oschlies, A., et al. 2018. Declining oxygen in the global ocean and
907   coastal waters. *Science*, 359(6371): eaam7240. doi: 10.1126/science.aam7240
908

909 Chabot, D. and Dutil, J.-D. 1999. Reduced growth of Atlantic cod in non-lethal hypoxic
910   conditions. *J. Fish. Biol.*, 55: 472-491. https://doi.org/10.1111/j.1095-
911   8649.1999.tb00693.x
912

913 Chambers, R. C. and Leggett, W. C. 1987. Size and age at metamorphosis in marine fishes – an
914   analysis of laboratory-reared winter flounder (*Pseudopleuronectes americanus*) with a
915   review of variation in other species. *Can. J. Fish. Aquat. Sci.*, 44(11): 1936-1947.
916   https://doi.org/10.1139/f87-238
917

918 Chapman, L. J. and McKenzie, D. J. 2009. Behavioral responses and ecological consequences.
919   In: *Fish Physiology, Vol. 27: Hypoxia*. (Ed. Jeffrey G. Richards, Anthony P. Farrell, and
920   Colin J. Brauner), pp. 25-77. San Diego: Academic Press.
921

922 Ciuhandu, C. S., Stevens, E. D., and Wright, P. A. 2005. The effect of oxygen on the growth of
923   *Oncorhynchus mykiss* embryos with and without a chorion. *J. Fish. Biol.*, 67: 1544-1551.
924   https://doi.org/10.1111/j.1095-8649.2005.00856.x

Claireaux, G. and Chabot, D. 2016. Responses by fishes to environmental hypoxia: integration through Fry's concept of aerobic metabolic scope. *J. Fish Biol.*, 88: 232-251. https://doi.org.10.1111/jfb.12833

Concannon, C. A., Cross, E. L., Jones, L. F., Murray, C. S., Matassa, C. M., McBride, R. S., and Baumann, H. 2021. Temperature-dependent effects on fecundity in a serial broadcast spawning fish after whole-life high CO_2 exposure. *ICES J. Mar. Sci.*, 78(10): 3724-3734. https://doi.org/10.1093/icesjms/fsab217

Cross, E. L., Murray, C. S., and Baumann, H. 2019. Diel and tidal pCO_2 x O_2 fluctuations provide physiological refuge to early life stages of a coastal forage fish. *Sci. Rep.*, 9: 18146. https://doi.org/10.1038/s41598-019-53930-8

Del Rio, A. M., Davis, B. E., Fangue, N. A., and Todgham, A. E. 2019. Combined effects of warming and hypoxia on early life stage Chinook salmon physiology and development. *Conserv. Physiol.*, 7(1): coy078. doi: 10.1093/conphys/coy078

DePasquale, E., Baumann, H., and Gobler, C. J. 2015. Vulnerability of early life stage Northwest Atlantic forage fish to ocean acidification and low oxygen. *Mar. Ecol. Prog. Ser.*, 523: 145-156. doi: 10.3354/meps11142

Desforges, J.-P. W., Sonne, C., and Dietz, R. 2017. Using energy budgets to combine ecology and toxicology in a mammalian sentinel species. *Sci. Rep.*, 7: 46267. doi: 10.1038/srep46267

Di Santo, V., Kenaley, C. P., and Lauder, G. V. 2017. High postural costs and anaerobic metabolism during swimming support the hypothesis of a U-shaped metabolism–speed curve in fishes. *Proc. Nat. Acad. Sci.*, 114(49): 13048-13053. https://doi.org/10.1073/pnas.1715141114

Diaz, R. J. and Rosenberg, R. 2008. Spreading Dead Zones and Consequences for Marine Ecosystems. *Science*, 321: 926-929. doi: 10.1126/science.1156401

Earhart, M. L., Blanchard, T. S., Harman, A. A., and Schulte, P. M. 2022. Hypoxia and High Temperature as Interacting Stressors: Will Plasticity Promote Resilience of Fishes in a Changing World? *Biol. Bull.*, 243: 149-170. https://doi.org/10.1086/722115

Evans, M. R., Grimm, V., Johst, K., et al. 2013. Do simple models lead to generality in ecology? *Trends in Ecology & Evolution*, 28(10): 578-583. https://doi.org/10.1016/j.tree.2013.05.022

Farrell, A. P. and Brauner, C. J. 2009. Fish Physiology, Vol. 27: Hypoxia. Academic Press, London.

970   Finn, R. N., Fyhn, H. J., and Evjen, M. S. 1995. Physiological energetics of developing embryos
971   and yolk-sac larvae of Atlantic cod (*Gadus morhua*). I. Respiration and nitrogen
972   metabolism. *Mar. Biol.*, 124: 355-369. https://doi.org/10.1007/BF00363909
973

974   Goussen, B., Rendal, C., Sheffield, D., Butler, E., Price, O. R., and Ashauer, R. 2020.
975   Bioenergetics modelling to analyze and predict the joint effects of multiple stressors:
976   Meta-analysis and model corroboration. *Sci. Total. Environ.*, 749: 141509.
977   https://doi.org/10.1016/j.scitotenv.2020.141509
978

979   Grear, J. S., O'Leary, C. A., Nye, J. A., Tettelbach, S. T., and Gobler, C. J. 2020. Effects of
980   coastal acidification on North Atlantic bivalves: interpreting laboratory responses in the
981   context of *in situ* populations. *Mar. Ecol. Prog. Ser.*, 633: 89-104.
982   https://doi.org/10.3354/meps13140
983

984   Gruber, J. 2011. Warming up, turning sour, losing breath: ocean biogeochemistry under global
985   change. *Phil. Trans. R. Soc. A*, 369: 1980-1996. https://doi.org/10.1098/rsta.2011.0003
986

987   Hamda, N. T., Martin, B., Poletto, J. B., Cocherell, D. E., Fangue, N. A., Van Eenennaam, J.,
988   Mora, E. A., and Danner, E. 2019. Applying a simplified energy-budget model to explore
989   the effects of temperature and food availability on the life history of green sturgeon
990   (*Acipenser medirostris*). *Ecol. Modell.*, 395: 1-10.
991   https://doi.org/10.1016/j.ecolmodel.2019.01.005
992

993   Hancock, J. R. and Place, S. P. 2016. Impact of ocean acidification on the hypoxia tolerance of
994   the woolly sculpin, *Clinocottus analis. Conserv. Physiol*. 4, cow040.
995   doi:10.1093/conphys/cow040
996

997   Heath, A. G. and Pritchard, A. W. 1965. Effects of severe hypoxia on carbohydrate energy stores
998   and metabolism in two species of fresh-water fish. *Physiol. Zool.*, 38(4): 325-334.
999   https://doi.org/10.1086/physzool.38.4.30152409
1000

1001   Holling, C. S. 1966. The strategy of building models of complex ecological systems. In: Systems
1002   Analysis in Ecology. (K. E. F. Watt, Ed.) Academic Press. Pp. 195-214.
1003

1004   Howarth, R., Chan, F., Conley, D. J., Garnier, J., Doney, S. C., Marino, R., and Billen, G. 2011.
1005   Coupled biogeochemical cycles: eutrophication and hypoxia in temperate estuaries and
1006   coastal marine ecosystems. *Front. Ecol. Environ.*, 9(1): 18-26. doi: 10.1890/100008
1007

1008   Jager, T. 2018. DEBkiss: A Simple Framework for Animal Energy Budgets. Version 2.0.
1009   Leanpub: https://leanpub.com/debkiss_book.
1010

1011   Jager, T., Martin, B. T., and Zimmer, E. I. 2013. DEBkiss or the quest for the simplest generic
1012   model of animal life history. *J. Theor. Biol.*, 328: 9-18.
1013   https://doi.org/10.1016/j.jtbi.2013.03.011
1014

Jager, T., Ravagnan, E., and Dupont, S. 2016. Near-future ocean acidification impacts maintenance costs in sea-urchin larvae: Identification of stress factors and tipping points using a DEB modelling approach. *J. Exp. Mar. Biol. Ecol.*, 474: 11-17. https://doi.org/10.1016/j.jembe.2015.09.016

Jager, T., Nepstad, R., Hansen, B. H., and Farkas, J. 2018. Simple energy-budget model for yolk-feeding stages of Atlantic cod (*Gadus morhua*). *Ecol. Modell.*, 385: 213-219. https://doi.org/10.1016/j.ecolmodel.2018.08.003

Jusup, M., Sousa, T., Domingos, T., Labinac, V., Marn, N., Wang, Z., and Klanjšček, T. 2017. Physics of metabolic organization. *Physics of Life Reviews*, 20: 1-39. https://doi.org/10.1016/j.plrev.2016.09.001

Kajimura, S., Aida, K., and Duan, C. 2005. Insulin-like growth factor-binding protein-1 (IGFBP-1) mediates hypoxia-induced embryonic growth and developmental retardation. *Proc. Nat. Acad. Sci.*, 102(4): 1240-1245. https://doi.org/10.1073/pnas.0407443102

Kajimura, S., Aida, K., and Duan, C. 2006. Understanding Hypoxia-Induced Gene Expression in Early Development: In Vitro and In Vivo Analysis of Hypoxia-Inducible Factor 1-Regulated Zebra Fish Insulin-Like Growth Factor Binding Protein 1 Gene Expression. *Mol. Cell. Biol.*, 26(3): 1142-1155. https://doi.org/10.1128/MCB.26.3.1142-1155.2006

Kamler, E. 2008. Resource allocation in yolk-feeding fish. *Rev. Fish. Biol. Fisheries*, 18: 143-200. https://doi.org/10.1007/s11160-007-9070-x

Klahre, L. E. 1997. Countergradient Variation in Egg Production Rate of the Atlantic Silverside *Menidia menidia*. [Master's thesis]. Stony Brook University.

Kooijman, S. A. L. M. 2010a. Dynamic Energy Budget Theory for Metabolic Organisation. Cambridge University Press, Cambridge.

Kooijman, S. A. L. M. 2010b. Comments on Dynamic Energy Budget Theory for Metabolic Organisation. Cambridge University Press, Cambridge.

Kooijman, S. A. L. M. 2018. Models in stress research. *Ecol. Complex.*, 34: 161-177. https://doi.org/10.1016/j.ecocom.2017.07.006

Kooijman, S. A. L. M., and Metz, J. A. J. 1984. On the dynamics of chemically stressed populations: The deduction of population consequences from effects on individuals. *Ecotoxicology and Environmental Safety*, 8(3): 254-274. https://doi.org/10.1016/0147-6513(84)90029-0

Kooijman, S. A. L. M., Baas, J., Bontje, D., Broerse, M., van Gestel, C. A. M., and Jager, T. 2009. Ecotoxicological Applications of Dynamic Energy Budget Theory. In: *Emerging Topics in Ecotoxicology, Vol. 2: Ecotoxicology Modeling* (Ed. Devillers, J.), pp. 237-259. Boston, MA: Springer. https://doi.org/10.1007/978-1-4419-0197-2_9

1061

Kooijman, S. A. L. M., Lika, K., Augustine, S., Marn, N., and Kooi, B. W. 2020. The energetic
basis of population growth in animal kingdom. *Ecol. Modell.*, 428: 109055.
https://doi.org/10.1016/j.ecolmodel.2020.109055

Kramer, D. L. 1987. Dissolved oxygen and fish behavior. *Environmental Biology of Fishes*, 18:
81-92. https://doi.org/10.1007/BF00002597

Landry, C. A., Steele, S. L., Manning, S., and Cheek, A. O. 2007. Long term hypoxia suppresses
reproductive capacity in the estuarine fish, *Fundulus grandis*. *Comp. Biochem. Physiol.
Part A: Mol. Integr. Physiol.*, 148(2): 317-323.
https://doi.org/10.1016/j.cbpa.2007.04.023

Lankford, T. E., Billerbeck, J. M., and Conover, D. O. 2001. Evolution of intrinsic growth and
energy acquisition rates. II. Trade-offs with vulnerability to predation in *Menidia
menidia*. *Evolution*, 55(9): 1873-1881. https://doi.org/10.1111/j.0014-
3820.2001.tb00836.x

Lavaud, R., Filgueira, R., and Augustine, S. 2019. The role of Dynamic Energy Budgets in
conservation physiology. *Conserv. Physiol.*, 9(1): coab083. doi:
10.1093/conphys/coab083

Lavaud, R., Filgueira, R., and Augustine, S. 2021. The role of Dynamic Energy Budgets in
conservation physiology. *Conserv. Physiol.*, 9(1): coab083. doi:
10.1093/conphys/coab083.

Letcher, B. H. and Bengtson, D. A. 1993. Effects of food density and temperature on feeding and
growth of young inland silversides (*Menidia beryllina*). *J. Fish Biol.*, 43: 671-686.
https://doi.org/10.1111/j.1095-8649.1993.tb01145.x

Lika, K., Kearney, M. R., Freitas, V., van der Veer, H. W., van der Meer, J., Mijsman, J. W. M.,
Pecqueries, L., and Kooijman, S. A. L. M. 2011. The "covariation method" for estimating
the parameters of the standard Dynamic Energy Budget model I: Philosophy and
approach. *J. Sea Res.*, 66(4): 270-277. https://doi.org/10.1016/j.seares.2011.07.010

Marques, G. M., Augustine, S., Lika, K., Pecquerie, L., Domingos, T., and Kooijman, S. A. L.
M. 2018. The AmP project: Comparing species on the basis of dynamic energy budget
parameters. *PLoS Comput. Biol.*, 14(5): e1006100.
https://doi.org/10.1371/journal.pcbi.1006100

Martin, B. T., Jager, T., Nisbet, R. M., Preuss, T. G., and Grimm, V. 2013. Predicting Population
Dynamics from the Properties of Individuals: A Cross-Level Test of Dynamic Energy
Budget Theory. *The American Naturalist*, 181(4): 506-519.
https://doi.org/10.1086/669904

Martin, B. T., Heintz, R., Danner, E. M., and Nisbet, R. M. 2017. Integrating lipid storage into general representations of fish energetics. *Journal of Animal Ecology*, 86: 812-825. https://doi.org/10.1111/1365-2656.12667

Maury, O., Poggiale, J.-C., and Aumont, O. 2019. Damage-related protein turnover explains inter-specific patterns of maintenance rate and suggest modifications of the DEB theory. *J. Sea Res.*, 143: 35-47. https://doi.org/10.1016/j.seares.2018.09.021

Maxime, V., Pichavant, K., Boeuf, G., and Nonnotte, G. 2000. Effects of hypoxia on respiratory physiology of turbot, *Scophthalmus maximus*. *Fish Physiology and Biochemistry*, 22: 51-59. https://doi.org/10.1023/A:1007829214826

May, R. M. 2001. Stability and Complexity in Model Ecosystems. 2nd Edition. Princeton University Press.

McBryan, T. L., Anttila, K., Healy, T. M., and Schulte, P. M. 2013. Responses to temperature and hypoxia as interacting stressors in fish: implications for adaptation to environmental change. *Integr. Comp. Biol.*, 53: 648-659. doi: 10.1093/icb/ict066

Middaugh, D. P. 1981. Reproductive Ecology and Spawning Periodicity of the Atlantic Silverside, *Menidia menidia* (Pisces: Atherinidae). *Copeia*, 1981(4): 766-776. https://doi.org/10.2307/1444176

Middaugh, D. P. and Lempesis, P. W. 1976. Laboratory spawning and rearing of a marine fish, the silverside *Menidia menidia menidia*. *Mar. Biol.*, 35: 295-300. https://doi.org/10.1007/BF00386640

Middaugh, D. P. and Hemmer, M. J. 1992. Reproductive Ecology of the Inland Silverside, *Menidia beryllina*, (Pisces: Atherinidae) from Blackwater Bay, Florida. *Copeia*, 1992(1): 53-61. https://doi.org/10.2307/1446535

Miller, S. H., Breitburg, D. L., Burrell, R. B., Keppel, A. G. 2016. Acidification increases sensitivity to hypoxia in important forage fishes. *Mar. Ecol. Prog. Ser.*, 549: 1-8. https://doi.org/10.3354/meps11695

Moreira, J. M., Candeias Mendes, A., Maulvault, A. L., Marques, A., Rosa, R., Pousão-Ferreira, P., Sousa, T., Anacleto, P., and Marques, G. M. 2022. Impacts of ocean warming and acidification on the energy budget of three commercially important fish species. *Conserv. Physiol.*, 10(1): coac048. https://doi.org/10.1093/conphys/coac048

Morrell, B. K. and Gobler, C. J. 2020. Negative Effects of Diurnal Changes in Acidification and Hypoxia on Early-Life Stage Estuarine Fishes. *Diversity*, 12: 25. doi: 10.3390/d12010025

Muller, E. B., Nisbet, R. M., and Berkley, H. A. 2010. Sublethal toxicant effects with dynamic energy budget theory: model formulation. *Ecotoxicology*, 19: 48-60. https://doi.org/10.1007/s10646-009-0385-3

38

Muller, E. B., Klanjšček, T., and Nisbet, R. M. 2019. Inhibition and damage schemes within the synthesizing unit concept of dynamic energy budget theory. *J. Sea Res.*, 143: 165-172. https://doi.org/10.1016/j.seares.2018.05.006

Murphy, C. A., Nisbet, R. M., Antczak, P., Garcia-Reyero, N., Gergs, A., Lika, K., Mathews, T., Muller, E. B., Nacci, D., Peace, A., Remien, C. H., Schultz, I. R., Stevenson, L. M., and Watanabe, K. H. 2018. Incorporating Suborganismal Processes into Dynamic Energy Budget Models for Ecological Risk Assessment. *Integr. Environ. Assess. Manag.*, 14(5): 615-624. doi: 10.1002/ieam.4063

Murray, C. S. and Baumann, H. 2018. You Better Repeat It: Complex $CO_2 \times$ Temperature Effects in Atlantic Silverside Offspring Revealed by Serial Experimentation. *Diversity*, 10: 69. doi: 10.3390/d10030069

[dataset] Murray, C., Baumann, H. (2018) $CO_2 \times$ temperature specific early life survival and growth of *Menidia menidia* assessed by 5 factorial experiments. Biological and Chemical Oceanography Data Management Office (BCO-DMO). (Version 05 April 2018) Version Date 2018-04-05. doi:10.1575/1912/bco-dmo.742200 [accessed 2022-03-30]

Murray, C. S. and Baumann, H. 2020. Are long-term growth responses to elevated pCO₂ sex-specific in fish? *PLoS ONE*, 15(7): e0235817. https://doi.org/10.1371/journal.pone.0235817

Murray, C. S., Fuiman, L. A., and Baumann, H. 2017. Consequences of elevated CO_2 exposure across multiple life stages in a coastal forage fish. *ICES J. Mar. Sci.*, 74(4): 1051-1061. doi: 10.1093/icesjms/fsw179

Nicieza, A. G. and Metcalfe, N. B. 1997. Growth compensation in juvenile Atlantic salmon: Responses to depressed temperature and food availability. *Ecology*, 78(8): 2385-2400. https://doi.org/10.1890/0012-9658(1997)078[2385:GCIJAS]2.0.CO;2

Niklitschek, E. J. and Secor, D. H. 2005. Modeling spatial and temporal variation of suitable nursery habitats for Atlantic sturgeon in the Chesapeake Bay. *Estuar. Coast. Shelf Sci.*, 64: 135-148. https://doi.org/10.1016/j.ecss.2005.02.012

Nilsson, G. E. and Östlund-Nilsson, S. 2008. Does size matter for hypoxia tolerance in fish? *Biol. Rev.*, 83: 173-189. https://doi.org/10.1111/j.1469-185X.2008.00038.x

Ninness, M. M., Stevens, E. D., and Wright, P. A. 2006. Removal of the chorion before hatching results in increased movement and accelerated growth in rainbow trout (*Oncorhynchus mykiss*) embryos. *J. Exp. Biol.*, 209: 1874-1882. https://doi.org/10.1242/jeb.02200

Nisbet, R. M., Gurney, W. S. C., Murdoch, W. W., and McCauley, E. 1989. Structured population models: a tool for linking effects at individual and population level. *Biol. J. Linn. Soc.*, 37: 79-99. https://doi.org/10.1111/j.1095-8312.1989.tb02006.x

Nisbet, R. M., Muller, E. B., Lika, K., and Kooijman, S. A. L. M. 2000. From molecules to
ecosystems through dynamic energy budget models. *Journal of Animal Ecology*, 69: 913-926.

Nonnotte, G., Maxime, V., Truchot, J. P., Williot, P., and Peyraud, C. 1993. Respiratory
responses to progressive ambient hypoxia in the sturgeon, *Acipenser baeri*. *Respir.
Physiol.*, 91: 71-82. https://doi.org/10.1016/0034-5687(93)90090-W

O'Donnell, J., Dam, H. G., Bohlen, W. F., Fitzgerald, W., Gay, P. S., Houk, A. E., Cohen, D. C.,
and Howard-Strobel, M. M. 2008. Intermittent ventilation in the hypoxic zone of western
Long Island Sound during the summer of 2004. *J. Geophys. Res.*, 113: C09025.
https://doi.org/10.1029/2007JC004716

Perry, S. F., Jonz, M. G., and Gilmour, K. M. 2009. Oxygen Sensing and the Hypoxic
Ventilatory Response. In: *Fish Physiology, Vol. 27: Hypoxia*. (Ed. J. G. Richards, A. P.
Farrell and C. J. Brauner), pp. 193-253. San Diego: Academic Press.

Polymeropoulos, E. T., Elliott, N. G., and Frappell, P. B. 2017. Hypoxic acclimation leads to
metabolic compensation after reoxygenation in Atlantic salmon yolk-sac alevins. *Comp.
Biochem. Physiol. A*, 213: 28-35. https://doi.org/10.1016/j.cbpa.2017.08.011

Pousse, É., Munroe, D., Hart, D., Hennen, D., Cameron, L. P., Rheuban, J. E., Wang, Z. A.,
Wikfors, G. H., and Meseck, S. L. 2022. Dynamic energy budget modeling of Atlantic
surfclam, *Spisula solidissima*, under future ocean acidification and warming. *Mar.
Environ. Res.*, 177: 105602. https://doi.org/10.1016/j.marenvres.2022.105602

Rabalais, N. N., Turner, R. E., Díaz, R. J., and Justić, D. 2009. Global change and eutrophication
of coastal waters. *ICES J. Mar. Sci.*, 66(7): 1528-1537.
https://doi.org/10.1093/icesjms/fsp047

Richards, J. G. 2009. Metabolic and Molecular Responses of Fish to Hypoxia. In: *Fish
Physiology, Vol. 27: Hypoxia*. (Ed. J. G. Richards, A. P. Farrell and C. J. Brauner), pp.
443-485. San Diego: Academic Press.

Richards, J. G. 2011. Physiological, behavioral and biochemical adaptations of intertidal fishes
to hypoxia. *J. Exp. Biol.*, 214: 191-199. https://doi.org/10.1242/jeb.047951

Robert, D., Shoji, J., Sirois, P., Takasuka, A., Catalán, I. A., et al. 2023. Life in the fast lane:
Revisiting the fast growth—High survival paradigm during the early life stages of fish.
Fish and Fisheries, 24: 863-888. https://doi.org/10.1111/faf.12774

Rombough, P. J. 1988. Respiratory gas exchange, aerobic metabolism, and effects of hypoxia
during early life. In: *Fish Physiology, Vol. 11: The Physiology of Developing Fish, Part
A: Eggs and Larvae*. (ed. W. S. Hoar and D. J. Randall), pp. 59-162. San Diego:
Academic Press.

Romoli, C., Jager, T., Trijau, M., Goussen, B., and Gergs, A. 2024. Environmental Risk Assessment with Energy Budget Models: A Comparison Between Two Models of Different Complexity. *Environ. Toxicol. Chem.*, 43(2): 440-449. doi: 10.1002/etc.5795

Russell, N. R., and Wootton, R. J. 1992. Appetite and growth compensation in the European minnow, *Phoxinus phoxinus* (Cyprinidae), following short periods of food restriction. *Environ. Biol. Fishes*, 34: 277-285. https://doi.org/10.1007/BF00004774

Schwemmer, T. G. 2023. Early Life Physiological and Energetic Responses of Atlantic Silversides (*Menidia menidia*) to Ocean Acidification, Warming, and Hypoxia. Doctoral dissertation. ProQuest Dissertations Publishing. State University of New York at Stony Brook, Stony Brook, NY.

Schwemmer, T. G., Baumann, H., Murray, C. S., Molina, A. I., and Nye, J. A. 2020. Acidification and hypoxia interactively affect metabolism in embryos, but not larvae, of the coastal forage fish *Menidia menidia*. *J. Exp. Biol.*, 223: jeb228015. doi: 10.1242/jeb.228015

Sibly, R. M., Grimm, V., Martin, B. T., Johnston, A. S. A., et al. 2013. Representing the acquisition and use of energy by individuals in agent-based models of animal populations. *Methods in Ecology and Evolution*, 4: 151-161. https://doi.org/10.1111/2041-210x.12002

Smallegange, I. M., Caswell, H., Toorians, M. E. M., and de Roos, A. M. 2017. Mechanistic description of population dynamics using dynamic energy budget theory incorporated into integral projection models. *Methods in Ecology and Evolution*, 8: 146-154. https://doi.org/10.1111/2041-210X.12675

Stevenson, L. M., Muller, E. B., Nacci, D., Clark, B. W., Whitehead, A., and Nisbet, R. M. 2023. Connecting Suborganismal Data to Bioenergetic Processes: Killifish Embryos Exposed to a Dioxin-Like Compound. *Environ. Toxicol. Chem.*, 42(9): 2040-2053. doi: 10.1002/etc.5680

Stierhoff, K. L., Targett, T. E., and Miller, K. 2006. Ecophysiological responses of juvenile summer and winter flounder to hypoxia: experimental and modeling analyses of effects on estuarine nursery quality. *Mar. Ecol. Prog. Ser.*, 325: 255-266. doi:10.3354/meps325255

Stierhoff, K. L., Targett, T. E., and Power, J. H. 2009. Hypoxia-induced growth limitation of juvenile fishes in an estuarine nursery: assessment of small-scale temporal dynamics using RNA:DNA. *Can. J. Fish. Aquat. Sci.*, 66(7): 1033-1047. https://doi.org/10.1139/F09-066

Sun, C.-F., Tao, Y., Jiang, X.-Y., and Zou, S.-M. 2011. IGF binding protein 1 is correlated with hypoxia-induced growth reduce and developmental defects in grass carp

(*Ctenopharyngodon idellus*) embryos. *Gen. Comp. Endocrinol.*, 172(3): 409-415. https://doi.org/10.1016/j.ygcen.2011.04.005

Tai, T. C., Sumaila, U. R., and Cheung, W. W. L. 2021. Ocean Acidification Amplifies Multi-Stressor Impacts on Global Marine Invertebrate Fisheries. *Front. Mar. Sci.*, 8: 596644. doi: 10.3389/fmars.2021.596644

Takasuka, A., Aoki, I., and Oozeki, Y. 2007. Predator-specific growth-selective predation on larval Japanese anchovy *Engraulis japonicus*. *Mar. Ecol. Prog. Ser.*, 350: 99-107. https://doi.org/10.3354/meps07158

Taylor, J. C. and Miller, J. M. 2001. Physiological performance of juvenile southern flounder, *Paralichthys lethostigma* (Jordan and Gilbert, 1884), in chronic and episodic hypoxia. *J. Exp. Mar. Biol. Ecol.*, 258: 195-214. https://doi.org/10.1016/S0022-0981(01)00215-5

Testa, J. M., Murphy, R. R., Brady, D. C., and Kemp, W. M. 2018. Nutrient- and Climate-Induced Shifts in the Phenology of Linked Biogeochemical Cycles in a Temperate Estuary. *Front. Mar. Sci.*, 5: 114. https://doi.org/10.3389/fmars.2018.00114

Thomas, P., Rahman, M. S., Kummer, J. A., and Lawson, S. 2006. Reproductive endocrine dysfunction in Atlantic croaker exposed to hypoxia. *Mar. Environ. Res.*, 62: S249-S252. https://doi.org/10.1016/j.marenvres.2006.04.031

Thomas, Y., Flye-Sainte-Marie, J., Chabot, D., Aguirre-Velarde, A., Marques, G. M., and Pecquerie, Laure. 2019. Effects of hypoxia on metabolic functions in marine organisms: Observed patterns and modelling assumptions within the context of Dynamic Energy Budget (DEB) theory. *J. Sea Res.*, 143: 231-242. https://doi.org/10.1016/j.seares.2018.05.001

Tian, Y.-M., Chen, J., Tao, Y., Jiang, X.-Y., and Zou, S.-M. 2014. Molecular cloning and function analysis of insulin-like growth factor binding protein 1a in blunt snout bream (*Megalobrama amblycephala*). *Dongwuxue Yanjiu*, 35(4): 300-306. 10.13918/j.issn.2095-8137.2014.4.300

Ton, C., Stamatiou, D., and Liew, C.-C. 2003. Gene expression profile of zebrafish exposed to hypoxia during development. *Physiol. Genomics*, 13(2): 97-106. https://doi.org/10.1152/physiolgenomics.00128.2002

Vanderplancke, G., Claireaux, G., Quazuguel, P., Madec, L., Ferraresso, S., Sévère, A., Zambonino-Infante, J.-L., and Mazurais, D. 2014. Hypoxic episode during the larval period has long-term effects on European sea bass juveniles (*Dicentrarchus labrax*). *Mar. Biol.*, 162: 367-376. https://doi.org/10.1007/s00227-014-2601-9

Wagenmakers, E.-J. and Farrell, S. 2004. AIC model selection using Akaike weights. *Psychon. Bull. Rev.*, 11(1): 192-196. https://doi.org/10.3758/BF03206482

1336 Wang, J., Yang, Y., Wang, Z., Xu, K., Xiao, X., and Mu, W. 2021. Comparison of effects in
1337   sustained and diel-cycling hypoxia on hypoxia tolerance, histology, physiology, and
1338   expression of clock genes in high latitude fish *Phoxinus lagowskii*. *Comp. Biochem.*
1339   *Physiol. A Mol. Integr. Physiol.*, 260: 111020.
1340   https://doi.org/10.1016/j.cbpa.2021.111020

1341

1342 Wei, L.-Z., Zhang, X.-M., Li, J., and Huang, G.-Q. 2008. Compensatory growth of Chinese
1343   shrimp, *Fenneropenaeus chinensis* following hypoxic exposure. *Aquacult. Int.*, 16: 455-
1344   470. https://doi.org/10.1007/s10499-007-9158-2

1345

1346 Wieser, W. 1995. Energetics of fish larvae, the smallest vertebrates. *Acta Physiol. Scand.*, 154:
1347   279-290. https://doi.org/10.1111/j.1748-1716.1995.tb09912.x

1348

1349 Williams, K. J., Cassidy, A. A., Verhille, C. E., Lamarre, S. G., and MacCormack, T. J. 2019.
1350   Diel cycling hypoxia enhances hypoxia tolerance in rainbow trout (*Oncorhynchus*
1351   *mykiss*): evidence of physiological and metabolic plasticity. *J. Exp. Biol.*, 222(14):
1352   jeb206045. https://doi.org/10.1242/jeb.206045

1353

1354 Wood, C. M. 2018. The fallacy of the P_{crit} – are there more useful alternatives? *J. Exp. Biol.*,
1355   221: jeb163717. doi: 10.1242/jeb.163717

1356

1357 Wu, R. S. S., Zhou, B. S., Randall, D. J., Woo, N. Y. S., and Lam, P. K. S. 2003. Aquatic
1358   Hypoxia Is an Endocrine Disruptor and Impairs Fish Reproduction. *Environ. Sci.*
1359   *Technol.*, 37(6): 1137-1141. https://doi.org/10.1021/es0258327

1360

1361 Zambonino-Infante, J. L., Mazurais, D., Dubuc, A., Quéau, P., Vanderplancke, G., Servili, A.,
1362   Cahu, C., Le Bayon, N., Huelvan, C., and Claireaux, G. 2017. An early life hypoxia event
1363   has a long-term impact on protein digestion and growth in juvenile European sea bass. *J.*
1364   *Exp. Biol.*, 220(10): 1846-1851. https://doi.org/10.1242/jeb.154922

1365

1366 Zhu, C.-D., Wang, Z.-H., and Yan, B. 2013. Strategies for hypoxia adaptation in fish species: a
1367   review. *J. Comp. Physiol. B*, 183: 1005-1013. https://doi.org/10.1007/s00360-013-0762-3

1368

1369   **Supplementary Figure**

1370
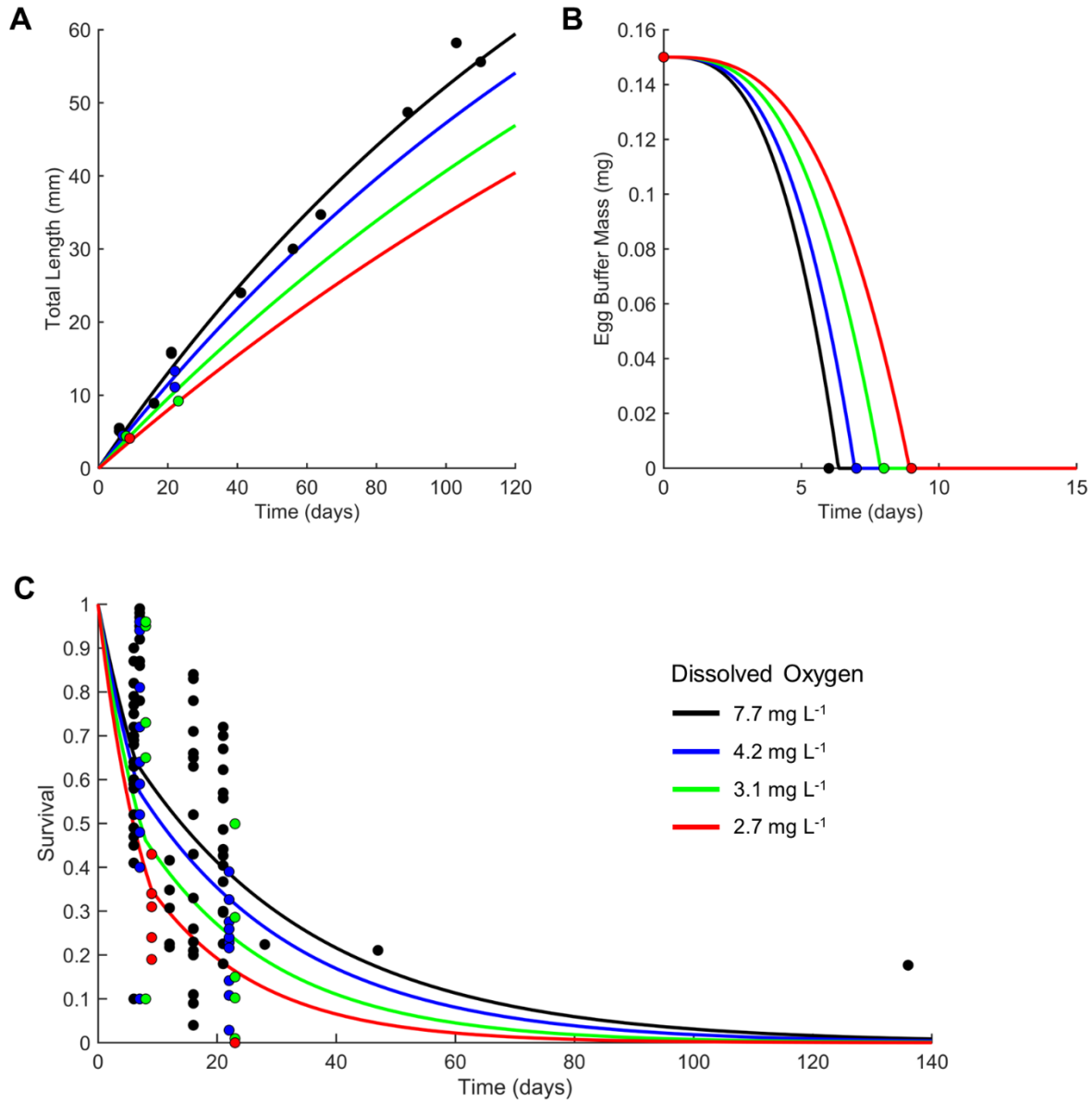
Figure S1. Best fit of DEBkiss model to all experimental data from four DO levels. The
model was fitted to early life data (embryos, larvae, and juveniles) and the best fitting model was
selected based on lowest AICc. (A) is total length (mm) over time (days), (B) is egg buffer mass
(mg) over time (days), and (C) is survival over time (days).

1375
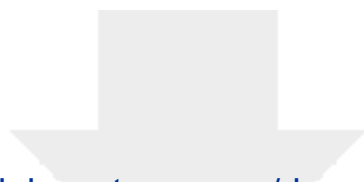
Click here to access/download
Supplementary material for online publication only
Supplementary Figure.docx
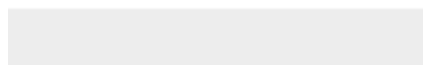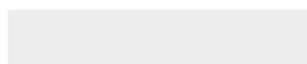
Declaration of interests

☒The authors declare that they have no known competing financial interests or personal relationships that could have appeared to influence the work reported in this paper.

☐The authors declare the following financial interests/personal relationships which may be considered as potential competing interests: